



Cite this: *Nanoscale Horiz.*, 2022,  
7, 1279

## Electrospun nanofibers for 3-D cancer models, diagnostics, and therapy

Ariane Erickson,<sup>†a</sup> Peter A. Chiarelli,<sup>†b</sup> Jianxi Huang,<sup>†a</sup>  
Sheeny Lan Levensgood<sup>a</sup> and Miqin Zhang<sup>†\*a</sup>

As one of the leading causes of global mortality, cancer has prompted extensive research and development to advance efficacious drug discovery, sustained drug delivery and improved sensitivity in diagnosis. Towards these applications, nanofibers synthesized by electrospinning have exhibited great clinical potential as a biomimetic tumor microenvironment model for drug screening, a controllable platform for localized, prolonged drug release for cancer therapy, and a highly sensitive cancer diagnostic tool for capture and isolation of circulating tumor cells in the bloodstream and for detection of cancer-associated biomarkers. This review provides an overview of applied nanofiber design with focus on versatile electrospinning fabrication techniques. The influence of topographical, physical, and biochemical properties on the function of nanofiber assemblies is discussed, as well as current and foreseeable barriers to the clinical translation of applied nanofibers in the field of oncology.

Received 12th July 2022,  
Accepted 31st August 2022

DOI: 10.1039/d2nh00328g

rsc.li/nanoscale-horizons

### 1 Introduction

Cancer remains a leading cause of death globally, and the second leading cause of death in the United States.<sup>1</sup> Projected incidence and death for the year 2022 are >1.9 million and >600 thousand, respectively.<sup>1</sup> To combat the morbidity and

mortality associated with cancer, innovative strategies from biochemistry, molecular genetics, and bioengineering disciplines have been implemented,<sup>2,3</sup> and have led to earlier diagnosis, improved targeted therapy, and increased rates of survival.<sup>4</sup> Nevertheless, a large number of preclinical discoveries fail to translate effectively towards human use and failure of clinical therapies in many forms of cancer remains high. The development of new drugs that target tumor-specific gene expression or the tumor microenvironment has been hindered, in part, by the relative scarcity of biomimetic *in vitro* drug screening models. Recently, 2D and 3D nanofibrous scaffolds, borrowed from regenerative medicine applications, have

<sup>a</sup> Department of Materials Science and Engineering, University of Washington, Seattle, WA 98195, USA. E-mail: mzhang@uw.edu

<sup>b</sup> The Saban Research Institute, University of Southern California, Children's Hospital Los Angeles, Los Angeles, CA 90027, USA

<sup>†</sup> These authors contributed equally to the manuscript.



Ariane Erickson

Ariane Erickson obtained her BS at Montana Tech of the University of Montana and received her PhD degree in Materials Science and Engineering and Nanotechnology from University of Washington in 2018. Her research has focused on electrospun nanofibers and polymeric scaffolds for tissue engineering and cancer research applications.



Peter A. Chiarelli

Peter Chiarelli is an Assistant Professor of Neurological Surgery at University of Southern California, and an attending neurosurgeon at Children's Hospital Los Angeles. He obtained his DPhil in Neuroscience at University of Oxford on a Rhodes Scholarship and earned his MD at the Harvard Medical School/Massachusetts Institute of Technology joint program in medicine. He went on to complete his neurosurgery residency and fellowship training at the University of Washington. His research has focused on treating pediatric tumors of the brain and spinal cord.

emerged as promising systems for cancer therapeutic screening, drug delivery, and diagnostics.

Nanomaterials, materials with at least one dimension < 100 nm, often exhibit properties that vary from those of the bulk material of similar chemical composition.<sup>5</sup> Progress in the field of nanomaterials design has continued since their emergence in the 1960s, including expanding applications in healthcare.<sup>6</sup> Biomedical applications may benefit from the potential of a nanomaterial scaffold to facilitate cellular functions and molecular processes, rather than simply acting as a passive agent in the presence of living tissue.<sup>7</sup> Nanoscaled fibers, for instance, mimic the support structure within the extracellular matrix of normal tissue, and are important materials in tissue engineering.<sup>8</sup> Nanofibers are also capable of simulating tumor stroma, providing a robust culture platform to better recapitulate the malignant/invasive tumor phenotype encountered *in vivo*. By representing more realistic tumor models, nanofibers may improve the accuracy of drug screening or the monitoring of tumor progression. Key attributes of nanofibers that render them advantageous for these applications include a high surface-to-volume ratio, variable porosity, inexpensive fabrication, and tunable characteristics of size/shape.<sup>9,10</sup>

The use of nanofiber materials for drug delivery has been studied extensively<sup>11–13</sup> with benefits of drug loading conferred by the aforementioned high surface area, and with research focused on delivery of diverse molecular ligands. Sustained ligand release from such materials is a key goal for their development, while minimizing unwanted bolus delivery/burst release of loaded drug compounds. Modification of the diameter, length, chemical composition, and surface functionalization of nanofibers has been shown to affect drug desorption rates, which can be matched with requirements for specific tissue-types or disease applications.<sup>13,14</sup> Surface functionalization of nanofibers is also useful for embedding targeting agents for detection of rare circulating tumor cells and tumor-associated biomarkers in biological fluids, rendering these materials useful for early cancer detection and point-of-care diagnosis.

In this review, we provide an overview of nanofiber design and fabrication utilizing the highly customizable technique of electrospinning. We discuss the applications of these electrospun fibers for (i) *in vitro* tumor modeling, (ii) drug delivery, and (iii) filtration/sensing (Fig. 1), along with the influence of topographical, physical, and biochemical nanoparticle properties on their function in these applications. This review also highlights current and foreseeable barriers to the clinical translation of these nanofiber assemblies and the outlook for future development in the field.

## 2 Synthesis of nanofibers by electrospinning

Over fifty various polymers and numerous solvents have been used for electrospinning fiber materials.<sup>15</sup> Selection of polymers and solvents determines solution conductivity and the interaction between the solvent and polymer, and thus nanofiber uniformity. The requirement for materials is also related to the corresponding research area. Biocompatibility must be taken into account for nanofiber materials used in 3-D tumor models,



**Jianxi Huang**

*Jianxi Huang received his MS in biomedical engineering from Duke University in 2020. He is currently a second year PhD student in materials science and engineering at the University of Washington. His current research interest lies in cancer treatment through nanomaterials and nanotechnology.*



**Sheeny Lan Levensgood**

*Sheeny Lan Levensgood received her PhD (2009) at the University of Illinois at Urbana-Champaign under the direction of Dr Amy Wagoner Johnson and Dr Russell Jamison. From there she was a Stem Cell and Regenerative Medicine Center postdoctoral research fellow at the University of Wisconsin-Madison working for Dr William Murphy (2009–2011). She was a postdoctoral research fellow in the Department of Materials Science and Engineering at the University of Washington working for Dr Miqin Zhang (2013–2016).*



**Miqin Zhang**

*Miqin Zhang is Kyocera Chair Professor of Materials Science & Engineering and Neurological Surgery, and adjunct professor in the Departments of Bioengineering, Radiology, and Orthopaedics & Sports Medicine at the University of Washington. She received her PhD from University of California at Berkeley. Her research focuses on nanomedicine for cancer diagnosis and treatment, biomaterials for tissue engineering, and biosensors for detection of chemical and biological agents.*



**Fig. 1** Schematic of three primary current applications for nanofibers in cancer research, including modeling of tumor microenvironment, drug delivery and cancer cell filtration and sensing. The high surface area of nanofibers can be advantageous for both cellular adhesion and interaction *in vitro*, as well as for the loading of molecular ligands for sustained drug delivery. The architecture and porosity of a nanofiber mesh can allow cell-specific binding and size-based filtration to separate circulating cancer cells from biological liquid samples such as blood and biological sensing of cancer-associated factors and genes.

anti-neoplastic drug delivery and cancer cell diagnostics. Hydrophilic polymers are preferred candidates for fast-dissolving delivery systems while hydrophobic polymers are adopted as a shell layer in delayed drug release system as a barrier from the penetration of medium into the core layer of drug.<sup>16</sup> Commonly used polymers for electrospun nanofibers in cancer research include synthetic polymers such as poly- $\epsilon$ -caprolactone (PCL), polylactic acid (PLA), poly(ethylene glycol) (PEG), poly(L-lactide) (PLLA), polylactic-co-glycolic acid (PLGA), polyurethane (PU), polyvinyl alcohol (PVA), polyethylene oxide (PEO), polyvinylpyrrolidone (PVP) and natural polymers such as cellulose, chitosan, hyaluronic acid, collagen and peptide.<sup>15–17</sup>

Numerous methods exist for nanofiber materials fabrication, including high-volume production methods: (i) melt fibrillation,<sup>18</sup> (ii) sea/island,<sup>19</sup> (iii) drawing,<sup>20,21</sup> (iv) dry spinning,<sup>22–24</sup> combinatory techniques: (i) force electrospinning,<sup>25,26</sup> and (ii) centrifugal electrospinning,<sup>27</sup> as well as more precise, small batch fabrication methods such as (i) nanolithography,<sup>28,29</sup> (ii) template directed synthesis,<sup>30–33</sup> (iii) phase separation,<sup>34</sup> (iv) vapor phase polymerization,<sup>35</sup> and (v) self-assembly.<sup>36–38</sup> Even with the abundance of options, electrospinning remains a dominant nanofiber construction technique because it allows for tight control of morphology and composition while using a cost-effective experimental apparatus and allowing for relatively rapid rates of production.<sup>9,10</sup>

## 2.1. Principles and methods

Electrospinning refers to the electrohydrodynamic technique for nanofiber assembly that utilizes a needle spinneret, a high



**Fig. 2** Schematic of electrospinning, displaying the spinneret, high voltage power supply, and grounded collector. The inset image shows the development of the Taylor cone profile within the fluid meniscus, as electrical potential is applied. By time +32 ms (upper right image), the droplet shape and fluid jet are stable resulting in consistent fiber production. Inset adapted with permission from ref. 41. Copyright 2008, Elsevier.

voltage power supply, and a grounded collector (Fig. 2). The spinneret reservoir is filled with an appropriate polymeric solution, colloidal emulsion, liquid suspension, or liquid-phase melted polymer, and is connected to a syringe pump or gravity feed to provide constant-flow egress of the solution. A high voltage field is applied between the spinneret and the grounded collector, which delivers an electrostatic force to the liquid that overcomes inherent surface tension and results in rapid extrusion of liquid filament from the spinneret tip. During this process, the rounded meniscus on the capillary tip of the spinneret acquires a conical profile (Taylor cone).<sup>39</sup> The charged polymer or analogous material filament is essentially “drawn” from the Taylor cone (conceptually similar to the process of spinning textiles), and is subjected to bending instability as the solvent evaporates, yielding solidification during fiber elongation. The elongation process promotes individual polymer chains aligning with one another.<sup>40</sup> The nanofiber produced from this tortuous polymer jet path forms a nonwoven fibrous mesh, and the resulting material is deposited layer-by-layer on the grounded collector.

A range of parameters related to the electrospinning apparatus can be modified to affect physical properties of the solid material product, such as the electric potential applied between spinneret tip and collector, the collector geometry, the spinneret-to-collector distance, and the bulk fluid flow rate.

Although increased voltage will promote elongation of the fiber and contribute to a reduction of fiber diameter, an increase in the solution feed rate will have the opposing effect of increasing nanofiber thickness. The spinneret configuration<sup>10</sup> can itself be changed to forms known as porous,<sup>42</sup> multi-spike,<sup>43</sup> coaxial,<sup>44</sup> gas-jet,<sup>45–47</sup> or bicomponents spinneret.<sup>48</sup> Example collector geometries include insulating gap or rotating drum collectors, both of which aim to increase nanofiber alignment.<sup>10,27</sup> Other collector configurations include grid-type,<sup>49</sup> edge-type,<sup>50</sup> rotary,<sup>10</sup> parallel electrode,<sup>27,51</sup> blade auxiliary electrode,<sup>52</sup> water bath,<sup>53</sup> and continuous collectors.<sup>27,54</sup> Nanofiber alignment and morphology are affected by the form of collector utilized in the apparatus.<sup>55,56</sup>

Variable ambient conditions in the intermediate region of electrospinning have a well-documented influence on fiber formation.<sup>45</sup> Elevated humidity will increase the presence of water adsorption during fiber solidification and may thus increase fiber porosity; elevated temperatures will diminish the viscosity of the solution and will yield nanofibers of decreased thickness. Chemical parameters of the primary liquid (molecular structure, concentration, molecular weight, solvent type) will influence viscosity, surface tension, conductivity, evaporation during filament extrusion, and the natural tendency of the material to self-assemble into an organized macromolecular architecture.<sup>57–59</sup> These properties have been shown to be intimately related to the diameter, morphology and uniformity of produced nanofibers.<sup>60</sup> Table 1 summarizes the these factors in the electrospinning process and the corresponding affected nanofiber properties.<sup>61</sup> Beyond single-constituent polymers, polymer blends have been utilized, as well as nanoparticle (NP)-impregnated or drug/ligand-impregnated polymers.<sup>61</sup> Non-polymeric carbon,<sup>62</sup> metals,<sup>48</sup> and ceramics<sup>63</sup> have also successfully produced uniform electrospun fiber structures.

For *in vitro* tumor modelling, nanofiber matrices with adequate pore size are required for cellular growth, migration and infiltration. Scaffolds synthesized by the layer-by-layer electrospun nanofiber deposition exhibit small pores that do not promote cellular infiltration.<sup>64</sup> Various post-processing or

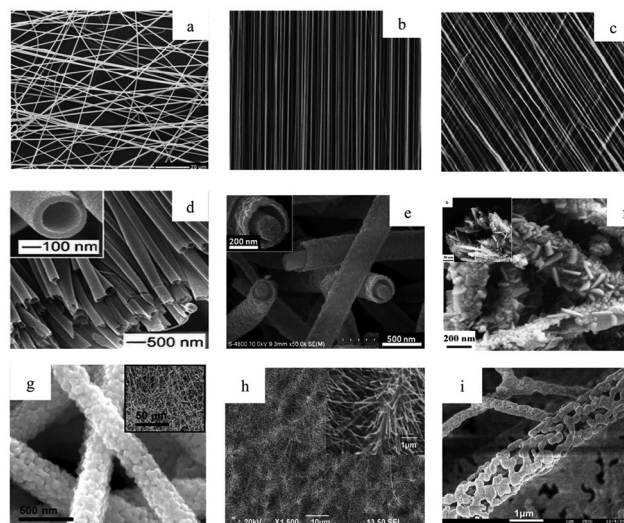


Fig. 3 Electrospun nanofibers as visualized using electron microscopy, including a range of fiber orientations (a) random, (b) aligned, (c) patterned, as well as diverse fiber morphologies, (d) hollow, (e) core-shell, (f) hybrid, (g) composite, (h) pine-needle, and (i) porous. Reprinted with permission from ref. 61. Copyright 2016, Royal Society of Chemistry.

modified processing approaches have been developed to increase the pore size and porosity of nanofiber scaffolds, including (1) freeze drying of parts of solution-containing electrospun nanofibers,<sup>65</sup> (2) gas-foaming of 2D electrospun nanofiber membranes,<sup>66</sup> (3) salt leaching,<sup>67</sup> (4) 3D weave technique,<sup>68</sup> and (5) hole forming by punching or laser ablation.<sup>69,70</sup>

A more detailed treatment of the electrospinning fabrication process can be found elsewhere.<sup>9,10,55,71–73</sup> Fig. 3 provides an example of the diverse nanofiber morphologies including visually identifiable differences in alignment, fiber spacing, diameter, and surface roughness. The mechanical stiffness and surface chemistry of these fibers have been observed to vary significantly as a result of their physical configuration, and in turn influence behavior of cells or biological fluids adjacent to the nanofibers.<sup>74</sup> Drugs and cells can be encapsulated in these

Table 1 Effects of experimental parameters/factors on nanofiber properties

Parameters/factors	Affected nanofiber properties	Influences
Voltage	Diameter	Increased voltage reduces fiber diameter
Solution feed rate	Diameter, porosity, shape	Increased solution feed rate results in greater nanofiber diameter
Spinneret-to-collector distance	Diameter	There are two opposing influences: (1) longer distance provides more time for solvent evaporation in the electric field and thus reduces fiber diameter; (2) longer distance results in lower electric field acceleration, and thus larger fiber diameter. The change in fiber diameter depends on the combined influences
Collector geometry	Alignment, morphology	Random, aligned, or braided fibers can be produced by various collector geometries
Humidity	Porosity	High humidity can lead to pores formation on fibers
Temperature	Diameter	Elevated temperature reduces the viscosity of the solution and yields nanofibers of decreased diameter
Polymer concentration	Diameter	Higher polymer concentration leads to larger nanofiber diameter
Polymer conductivity	Diameter	Higher polymer conductivity leads to smaller nanofiber diameter
Polymer molecular weight	Morphology, uniformity	High uniformity is seen in polymers with high molecular weight

constructs,<sup>75,76</sup> and the nanofiber surface can be further functionalized for medical screening/diagnostic purposes.<sup>77</sup> While this review will focus on applications to cancer medicine,<sup>78,79</sup> there exist diverse non-oncologic applications of these materials, for instance cosmetics, tissue engineering,<sup>80–82</sup> energy storage,<sup>83,84</sup> catalysis,<sup>85</sup> and air filtration.<sup>86,87</sup>

### 3. Nanofibers for *in vitro* tumor models

Neoplasm, which refers to abnormal growth of cells, is subdivided into benign and malignant forms. Cancer metastasis in the malignant form occurs *via* an interplay of biological processes, whereby neoplastic cells exhibit the ability to detach from extracellular matrix at their site of origin, migrate to a new site *via* hematogenous, lymphatic, or contiguous spread, and to establish nutrient supply and a favorable microenvironment at their destination. The process typically requires cells to traverse the vascular endothelium.<sup>88,89</sup> Although metastasis has been extensively studied, the ability to intervene clinically through manipulation of metastatic pathways remains somewhat limited. A lack of biomimetic tumor models that faithfully represent cancer metastasis is believed to be one of the main reasons for the high failure rate in translational oncologic drug discovery.<sup>90</sup>

Conventional *in vitro* culture technique commonly includes cells grown in 2-dimensional (2D) adherent monolayer configuration on a substrate such as polystyrene. Compared to cells within tumors that are sustained in 3-dimensions by a heterogeneous composite of adjacent tumor and stromal cells, as well as tumor-specific extracellular matrix (ECM), cells grown in a 2D configuration have larger contact area with the flat substrate and surrounding biological media. As a result, these lab-grown specimens tend to polarize and potentially lose normal physiological characteristics, resulting in dampening of the invasive phenotype.<sup>91</sup> To enhance biological relevance, organotypic tissue slice assays can be used to capture tumor cell interactions with relevant support cells and structural compounds in the stroma.<sup>92</sup> While these models are more relevant to the complex tissue microenvironment, organotypic assays have the disadvantage of being labor-intensive, and time-limited in their utility before tissue necrosis occurs and cell behavior/migratory patterns change.

In recent years a decisive shift has occurred away from strict reliance on monolayer/organotypic culture models, toward reproducible biomaterial-based platforms that can mimic the 3D tumor niche.<sup>93</sup> Constructs made of electrospun nanofibers present a significant potential advantage over conventional 2D monolayer culture as the fibrous topography can be designed to mimic native tumor stroma.<sup>94,95</sup> Nanofibers may also be fabricated from polymeric components found in the native tumor ECM. Another type of materials, hydrogel, also recently receives increasing research interest for developing 3D cancer culture models due to their biomimetic flexibility and biocompatibility. Compared to hydrogels, nanofiber scaffolds possess a large surface area to volume ratio and porosity that allows high

loading of physiological molecules, which have been perceived as a better mimicry of tumor ECM.<sup>96</sup>

Fibrous topography plays a significant role in mediating neoplastic invasion and metastasis. For instance, anisotropically oriented intracerebral white matter fibers can act as directional channels for invasion in primary brain cancers.<sup>97</sup> The topography of white matter is associated with upregulated cellular motility and consequent migratory behavior in high-grade glioma.<sup>98</sup> It has been suggested that the topography of the white matter may act as a pathway of least resistance for local brain tissue invasion, independent of any additional contribution from ECM neurotrophic growth factors or adhesion molecules.<sup>99</sup> Aligned collagen bundles also influence directional spread for soft tissue neoplasms such as breast cancer.<sup>100</sup> It has been shown that breast cancer cells preferentially invade along aligned tumor-associated collagen signature-3 (TAC-3) fibers, which are distributed perpendicular to the tumor boundary. Nanoscaled surface characteristics and the topography of nanofibers alone without surface functionalization have demonstrated effects on regulation of cell behavior such as adhesion, proliferation, alignment, and orientation, as well as on their genetic expression profile.<sup>98,101</sup>

Nanofiber platforms that mimic tumor microenvironmental cues can assist in modelling of disease progression *in vitro*. With accumulating knowledge of the feedback between the tumor microenvironment and cancer progression, efforts have emerged toward therapeutically suppressing the metastatic potential of highly migratory cancer types, which could transform a high-grade neoplasm to one that displays limited migrational behavior or invasiveness.<sup>98</sup> Nanofiber platforms can be utilized for high-throughput preclinical screening of anti-invasive therapies<sup>102</sup> and synchronize well with downstream assays including western blotting, immunostaining, live cell imaging, and RT-PCR.

#### 3.1. Influence of nanofiber alignment

The anisotropy of the fibrous matrix within tumor tissue has been observed to contribute to the upregulation of a migratory cell phenotype capable of invasion into healthy tissue. Cancer cells grown on nanofibers with variably aligned fibrous matrix have been found to display phenotypic properties (morphology, invasiveness, estimated histologic tumor grade) that closely match explanted tumor samples whose stromal fiber alignment is comparable.<sup>92</sup> Fig. 4 shows work by Nelson *et al.*,<sup>103</sup> who compared morphology of MDA-MB-231 human breast cancer cells cultured on flat tissue culture polystyrene (TCPS) with the morphology of cells cultured on randomly-oriented and aligned PCL nanofiber scaffolds. Cells cultured on TCPS (Fig. 4a and d) exhibited a rounded, spherical shape. Conversely, cells cultured on aligned nanofibers (Fig. 4c and f) displayed a more elongated spindle-like morphology, characteristic of cells with a highly invasive phenotype. Both spherical and highly elongated cells were found on randomly-oriented nanofibers (Fig. 4b and e). Further comparing breast cancer cells on aligned nanofibers with explanted samples, the authors found that tissue resected from tumor-bearing mice displayed a large number of collagen fibers with radial alignment towards the tumor-stroma boundary (Fig. 4g and h). Similar associations between nanofiber alignment

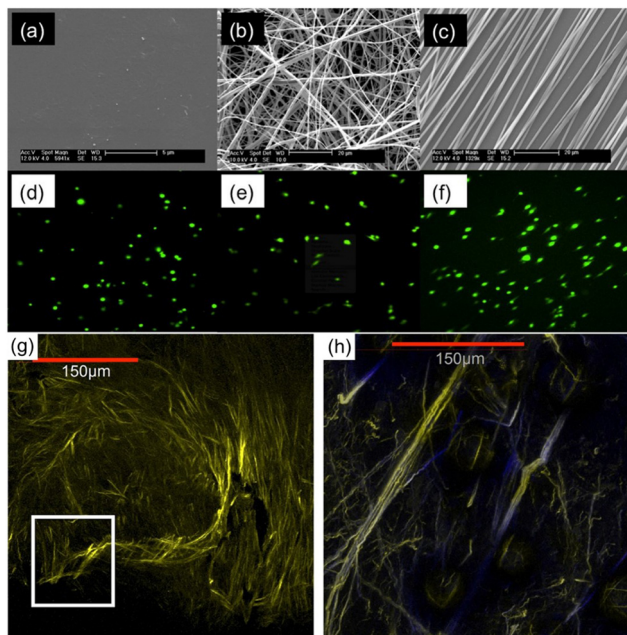


Fig. 4 Scanning electron microscopy (SEM) images displaying surface morphology of (a) TCPS plate, (b) randomly-oriented nanofibers, and (c) aligned nanofibers. Confocal images of MDA-MB-231 cells cultured on (d) TCPS, (e) randomly-oriented nanofibers, and (f) aligned nanofibers. Multiphoton microscopy images showing (g) dense collagen fibers around the central core of an explanted MDA-MB-231 xenograft breast tumor, and (h) radially aligned collagen fibers invading the tumor-stroma boundary. Reprinted with permission from ref. 103. Copyright 2014, Creative Commons Licence, <https://creativecommons.org/licenses/by/4.0/>.

and cell morphology were observed for other breast cell lines (e.g. MCF-10A and MCF),<sup>103</sup> as well as other cancer cell-types (glioma U251, U87) cultured on PCL nanofibers.<sup>94,95</sup>

Increased motility has been observed in cells on aligned nanofibers compared to randomly-oriented nanofibers. In a glioblastoma multiforme (GBM) culture model using aligned nanofiber scaffolds,<sup>94</sup> cell dispersion/migration along the nanofiber long axis was 6-fold greater than spatial dispersion perpendicular to this axis. The same group showed that c neurospheres deposited on randomly oriented nanofibers showed minimal departure of cells from the primary spheroid, with neurospheres retaining their size and shape over 20 hours.<sup>94</sup>

To study the influence of a patterned nanofiber substrate alignment on pathologic tumor cell migration at the genetic level, Beliveau *et al.* compared glioblastoma multiforme (GBM) cells cultured on aligned nanofibers with those grown on randomly oriented nanofibers as well as smooth surfaces. The group showed that GBM cell growth on an aligned nanofiber surface was correlated with reduced cytoskeletal stiffness, which allowed tumor cells to acquire greater deformational capability and increased predisposition to invasive behavior within the surrounding ECM *via* upregulation of key migratory genes. An increase in expression of *SNAI1* and *NOTCH1* and a downregulation in *CDK20* and *CCND1* was noted in cells cultured on aligned fibers.<sup>104</sup> Agudelo-Garcia *et al.* reported that GBM cells cultured on aligned polycaprolactone (PCL) 3D

nanofiber scaffolds showed a substantial increase in expression of *STAT3*, a known driver of glioma progression.<sup>105</sup>

### 3.2. Influence of nanofiber diameter

The average axonal diameter within human brain white matter is less than 1 μm; the diameter can range from 0.2 to 9 μm, and differs between intracranial white matter locations and between individuals.<sup>106</sup> Variation of electrospinning mechanical parameters and chemical solution properties (as described in Section 2.1) allows fabrication of nanofibers in diameter between tens of nanometers to microns. The effect of fiber size on breast cancer cell was analyzed by Rabionet *et al.*<sup>107</sup> MDA-MB-468 breast cancer cells exhibited a higher cell growth rate and a stronger cytoplasmic elongation on electrospun scaffolds with 700 nm PCL nanofibers than those with 300 nm nanofibers. Kievit *et al.* studied the effect of fiber size on brain cancer cell behavior, using aligned chitosan-polycaprolactone (C-PCL) nanofiber mats with fiber diameters of 200 nm, 400 nm, and 1.1 μm.<sup>95</sup> Cultured U87 GBM cells were observed to extend processes and align with the nanofiber long axis (Fig. 5a). Extent of GBM cellular migration was the greatest using 400 nm diameter nanofibers. GBM cultured with 200 nm and 400 nm aligned fibers both resulted in overexpression of invasion-related genes *β-catenin*, *SNAI1*, *STAT3*, *TGF-β*, and *TWIST* after 24 hours in culture, suggestive of mesenchymal-like transition in these cells. The distribution of intracellular endosomes in these cultures

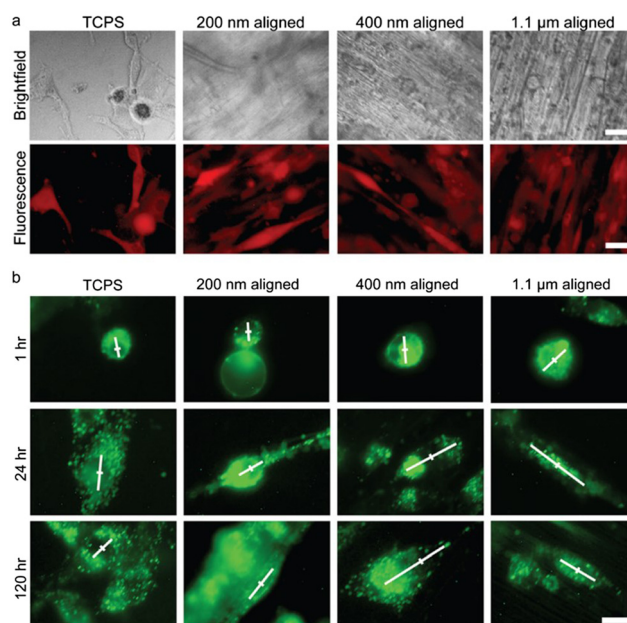


Fig. 5 U87 GBM cells cultured on variable-diameter aligned chitosan-PCL (C-PCL) nanofibers and 2-D TCPS plates for 120 hours. (a) RFP transfected (red) GBM cells viewed under brightfield (top panel) and fluorescence imaging (bottom panel). Scale bar represents 20 μm. (b) GBM cells with diol-stained membranes immediately after seeding on aligned C-PCL nanofibers of variable diameters. White lines convey principal direction and extent of endosomal distribution. The center of the cell is marked with a perpendicular line for reference. Scale bar represents 10 μm. Reprinted with permission from ref. 95. Copyright 2013, John Wiley and Sons.

was also investigated with respect to nanofiber diameter, as endosomal distribution is affected by cellular signaling pathways and can reflect changes in cell polarization that are involved in maintenance of cancer stem-like behavior. The asymmetry of endosomal distribution was found in cells cultured with 200 and 400 nm nanofibers, and was greatest in the 400 nm condition (Fig. 5b). As noted by the authors, the short time in culture required to observe these effects on gene expression and cellular polarization increased the utility of such an assay for drug screening applications.

### 3.3. Influence of nanofiber stiffness

Structural stiffness of the tumor microenvironment has been associated with cancer progression and metastatic behavior.<sup>108</sup> Rao *et al.* utilized core-shell nanofibers to fabricate materials with consistent surface chemistry but variable stiffness (conferred by

the core) to investigate the influence of mechanical stiffness of surrounding structures on GBM cell motility (Fig. 6).<sup>109</sup> Owing to the variation in core composition, the overall nanofiber scaffold elastic modulus could be altered from low stiffness (2 MPa for PCL-gelatin core) to medium (8 MPa for PCL core) and high stiffness (29 MPa for poly(ether sulfone) (PES)-PCL core; 33 MPa for polydimethylsiloxane (PDMS)-PCL core). Highest migration speed was observed using the nanofibers with an intermediate elastic modulus of 8 MPa. Cells cultured on nanofibers with a higher and lower elastic modulus displayed comparatively delayed migration, with the nanofibers of the lowest stiffness associated with slowest migration. Slow migration on softer substrates has been previously attributed to lowered resistance to cell-generated traction forces. Genetic expression in glioma has also been correlated with elastic modulus; decreased expression of FAK and MCL2 (genes implicated in glioma cellular migration) was observed using soft nanofiber substrates (PCL-gelatin).<sup>109,110</sup>

Table 2 summarizes experimental nanofiber parameters that have demonstrated effects on cellular migration. Nanofiber chemical composition, orientation, stiffness, and diameter are specified in cases where they are included as experimental variables, with cell type and tumor type also listed for reference.

## 4. Nanofibers for drug delivery

Achieving sustained therapeutic drug concentrations within or near a tumor site is a notable objective in translational oncology research.<sup>113,114</sup> Local delivery has the potential to decrease systemic toxicity of chemotherapeutics, and can increase the

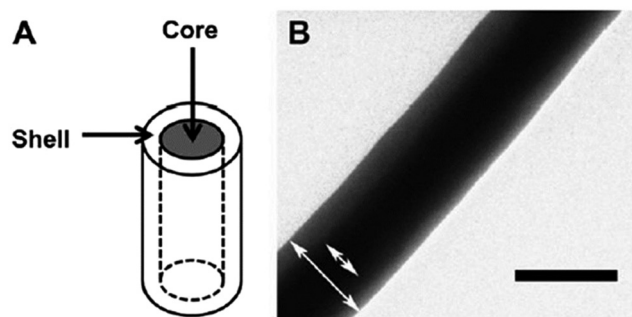


Fig. 6 Nanofiber comprised of PDMS core and PCL shell. (a) Schematic and (b) TEM image of core-shell configuration. Scale bar represents 0.2  $\mu\text{m}$ . Reprinted with permission from ref. 109; Copyright (2013), Elsevier.

Table 2 Summary of effects on migration by cell type, using multiple nanofiber platforms

Nanofiber type	Cell type (tumor type)	Average migration velocity ( $\mu\text{m h}^{-1}$ )	Comment	Ref.
PCL	U251 (brain tumor)	Aligned: $11.7 \pm 0.7$ ; <sup>b</sup> $4.2 \pm 0.39$ <sup>ab</sup> Random: $5.3 \pm 0.3$ ; <sup>b</sup> $0.8 \pm 0.08$ <sup>ab</sup>	Net distance cells travelled was 5 $\times$ greater on aligned nanofibers than on random nanofibers	94
PCL-Collagen	PANC-1 (pancreatic tumor)	Aligned: $\sim 10.5$ Random: $\sim 5.4$ Orthogonal: $\sim 5.4$	Aligned nanofibers promoted the cell migration, compared to random and orthogonal ones	111
Chitosan-PCL	U-87 MG (brain tumor)	TCPS: $35 \pm 14$ <sup>c</sup> 200 nm: $87 \pm 33$ <sup>c</sup> 400 nm: $40 \pm 12$ , <sup>c</sup> $13 \pm 3$ , <sup>d</sup> $2.5 \pm 1$ <sup>a</sup> 1100 nm: $60 \pm 15$ <sup>c</sup>	400 nm fibers yielded the highest median velocity	95
PCL core + chemokine (CXCL12) gel	MCF-10A, MCF-7, MDA-MB-231 (breast tumor)	MCF-10A: $3.1 \pm 5$ (random), $11.31 \pm 4$ (aligned) MCF-7: $7.1 \pm 5$ (random), $15.26 \pm 13$ (aligned) MDA-MB-231: $11.2 \pm 6.1$ (random), $32.3 \pm 13$ (aligned)	Increased migration rate was seen on aligned nanofibers compared to random nanofibers across all cell lines. Cell migration rate varied with cell type.	103
PCL core + ECM shell (varying biochemistry)	OSU-2 (brain tumor)	PCL-HA: $\sim 6$ PCL, PCL-collagen, PCL-matrigel: $\sim 11$ (all similar)	HA negatively impacted cell migration	109
PCL shell + varying core (varying stiffness)	OSU-2 (brain tumor)	Gelatin-PCL (2 MPa): $\sim 3.5$ PCL (8 MPa): $\sim 11$ PDMS-PCL (30 MPa): $\sim 6.3$ PES-PCL (30 MPa): $\sim 5.8$	Tumor cell migration speed is strongly correlated with nanofiber mechanics	109
PS <sup>e</sup>	DBTRG-05MG (brain tumor)	Flat: $\sim 26$ SS: $\sim 58$ DS: $\sim 45$	Cells on DS fibers migrated faster than on flat surfaces but slower and spread more versus on SS fibers	112

<sup>a</sup> Effective velocity. <sup>b</sup> Mean  $\pm$  SEM. <sup>c</sup> Maximum velocity. <sup>d</sup> Median velocity, hyaluronic acid (HA), polystyrene (PS), highly aligned parallel single suspended fibers (SS), orthogonally arranged double suspended fibers (DS). <sup>e</sup> STEP fabricated fibers.

length of time that a sufficient drug dosage persists within tumor tissue. As tumor recurrence often occurs near the margin of a surgically resected primary tumor, the use of brachytherapeutic or localized delivery approaches within the tumor bed has gained wide clinical acceptance.<sup>115,116</sup> In high-grade intracranial neoplasms such as GBM,<sup>117–119</sup> implanted regional drug delivery may also have the benefit of bypassing the blood brain barrier (BBB).<sup>120</sup> Modern advances in drug delivery have occurred with the design of micro/nanoparticles, which can be delivered systemically or locally *via* convection-enhanced delivery.<sup>7,116,117,121</sup> Nanoparticle can be administered intravascularly, which does not require surgery at the tumor site. However, short circulation time and possible off-target effects limit the nanoparticle-based treatment outcome. Hydrogel can be injected into the tumor site or cavity after surgical resection of solid tumor for topical drug release. But rapid drug release takes place in hydrogels due to their high water content and large pore sizes. Current clinical approaches also include the use of drug-eluting wafers or discs, which may be implanted in a resection bed at the time of open surgery. These technologies (both particle and implant delivery platforms) still possess limitations owing to low relative surface area, rates of polymer degradation,<sup>116</sup> and phenomena of initial burst release resulting in systemic or local toxicity.<sup>117,122</sup> Electrospun nanofibers hold promise as delivery platforms for localized drug release due to the relatively facile nature of drug incorporation during the process of electrospinning, as well as the large surface area, porous architecture, and tunable material properties of the nanofibers themselves.

#### 4.1. Drug incorporation methods

Incorporation of therapeutic compounds into nanofibers can occur during or after the electrospinning process. Modification of nanofiber material properties can be performed to alter the dynamics of drug loading. Variation of polymer type and concentration/viscosity, as well as resulting nanofiber diameter, porosity, and surface functionalization will affect drug loading and release profiles. Release kinetics are influenced by diffusion/desorption of the drug from a stable construct, or by degradation of the polymer construct itself.<sup>81,123,124</sup> The chosen method of incorporation will affect the mode and degree to which a ligand is intercalated within the final construct. Antibiotics, proteins, DNA, siRNA, growth factors, and living cells have been integrated with nanofibers *via* incorporation techniques including encapsulation, emulsion, surface adsorption/immobilization, and coaxial electrospinning, as described in Fig. 7.<sup>123</sup>

Drug loading will be affected by solubility of a treatment molecule in the polymer solution itself. Altering the drug incorporation method will often change the drug release profile.<sup>125</sup> Encapsulation is a conceptually straightforward method, involving mixing/co-solubilization of drug and polymer together, followed by electrospinning with a single spinneret. Standard solubility principles present expected limitations to this method, and hydrophobicity will affect the compatibility of matched drug-polymer solution pairs.<sup>126</sup> These limitations may be overcome using alternative methods such as coaxial electrospinning or emulsion electrospinning.

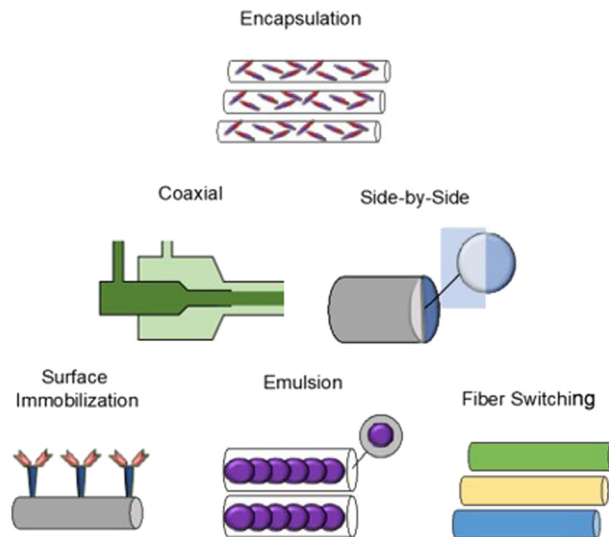


Fig. 7 Schematic illustrating common drug incorporation methods for nanofiber drug delivery, including encapsulation, coaxial electrospinning, side-by-side electrospinning, surface immobilization, emulsion electrospinning, and fiber switching.

Modifications in the configuration of the electrospinning hardware have been performed to generate novel nanofiber designs for drug delivery. Coaxial electrospinning, resulting in “core-shell” drug-nanofiber composites, is the combination of two polymer solutions using a co-axial double-nozzle spinneret.<sup>127</sup> The core polymer solution is injected within the shell polymer solution leading to a continuously coated nanofiber. Coaxial electrospinning allows blended nanofiber properties, and nanofibers can be constructed from a combination of materials that would have otherwise been poorly compatible by solubility alone.<sup>128</sup> The technique has been extended to tri-axial electrospinning (3 layers), with the potential for increasingly precise kinetics of controlled drug release.<sup>129</sup> Similar to coaxial electrospinning, side-by-side electrospinning also includes a modified nozzle configuration to combine multiple agents within the same fiber. The side-by-side nozzle has two adjacent ports, each with independent polymer solutions that are allowed to merge with one another in a common capillary channel.<sup>130</sup> Side-by-side fibers can combine dissimilar polymer solutions, and have the added benefit that both polymers may directly contact the surrounding environment.<sup>131</sup>

Fiber switching, another electrospinning method, uses multiple polymer solutions in a co-extrusion fashion, and results in a nanofiber meshwork containing contiguous fiber types of varying composition or drug concentration. Constructs synthesized by fiber switching have provided sustained release of a drug over time periods ranging from days to months.<sup>132</sup> Such long composite release phases occur by tailoring the polymer degradation rate used for individual fibers, tailoring the amount of drug loaded, and combining materials with overlapping release phases into adjacent portions of the nanofiber construct. Using a rodent orthotopic brain tumor model,<sup>132</sup> PLGA-PLA-PCL nanofibers fabricated by fiber switching and loaded with TMZ (Fig. 8) were implanted, with





**Fig. 8** TMZ-Loaded PLGA-PLA-PCL nanofiber implant for GBM treatment. (a) Photograph and (b) SEM image of 20 wt% TMZ-loaded nanofibers displaying flexibility and fibrous morphology. (c) Energy dispersive spectroscopy (EDS) map of tmz integration into nanofibers exhibits uniformity of drug distribution. (d) Drug release rate of implant tested in tumor-bearing rat brain over 30 days. Reprinted with permission from ref. 132. Copyright 2017, Creative Commons Licence, <https://creativecommons.org/licenses/by/4.0/>.

sustained drug release demonstrated over 30 days. After long term implantation of these nanofibers, increased survival of the animals was observed (85.7% survival at 4 months compared to 0% survival at 2 months in control condition), along with absence of tumor progression over this timeframe. Comparable implanted nanofibers designed to provide shorter 1 week drug release in the same tumor model yielded a lower survival rate of ~40% at 4 months, with median survival of ~2.5 months.

Emulsion electrospinning is a method designed to overcome barriers to the combination of hydrophobic and hydrophilic drugs in a single nanofiber. Organic solvent is conventionally used to dissolve the polymer, and drug is solubilized separately, with the otherwise immiscible solutions emulsified with the assistance of a surfactant.<sup>133</sup> Upon electrospinning, this micellar

mixture develops a boundary around the polymer, due to the rapid evaporation of organic solvent, resulting in increased polymer solution viscosity. The drug may either distribute throughout the boundary, or accumulate as a separate core within the formed polymer nanofibers, a configuration that can be altered depending on ligand molecular weight, difference in hydrophobicity, choice of surfactant, solution conductivity, solution flow rate and polymer viscosity.<sup>134</sup> Resulting emulsion nanofibers can have controlled release kinetics that are influenced by the fiber architecture and distribution of drug within the final construct. Emulsion techniques have been examined for the delivery of antineoplastic small-molecule drugs, and for functional gene delivery to tumors.<sup>135,136</sup>

Nanofibers with a surface-immobilized functional agent can be generated with an additional process stage, added after fabrication to the fiber base structure.<sup>123</sup> Techniques including physical adsorption (*e.g.* electrostatic surface coating, layer-by-layer deposition), chemical attachment (*e.g.* polymerization, mineralization, chemical surface conjugation), or chemical vapor/molecular layer deposition can be used to immobilize a separate chemical entity on the nanofiber surface. These fibers have been constructed with preserved surface agent bioactivity, while maintaining appropriate physical integrity of the nanofiber.<sup>137</sup> With a single layer of surface-bound drug, release kinetics are relatively more rapid compared to release kinetics of nanofiber-internalized drug, rendering these constructs more appropriate for applications where rapid release is desirable.<sup>96</sup> Surface immobilization has so far been a promising technology for proteins and growth factors, whose presentation into cell culture can be useful for *in vitro* drug screening models and cellular detection.<sup>123</sup> A synopsis of recent drug incorporation studies is provided in Table 3, specifying loading methods, nanofiber materials, and chosen treatment compound. Additional sources are available in the literature focusing on a more exhaustive technical treatment of drug-loading techniques.<sup>11,81,138</sup>

#### 4.2. Influence of nanofiber physical properties on drug release

Features of nanofiber macrostructure including intralayer fiber diameter, density, fiber orientation, and layer-by-layer design

**Table 3** Nanofiber incorporation methods

Nanofiber type	Drug	Loading method	Target cancer type	Release period of time	Comments	Citation
PLGA/PLA	PTX	Encapsulation	C6 (brain cancer cell)	Less than 50% of sustained drug release over 80 days <i>in vitro</i>	Fiber sheets showed a higher initial burst release than fiber discs. Nanofibers exhibited a higher release rate than microfibers	116
PLGA/PLA/PCL	TMZ	Encapsulation	U87MG and C6 (brain cancer cell)	Less than 20% of sustained drug release over 30 days <i>in vitro</i>	Drug release profile varied with different polymer blend ratios (PLGA : PLA : PCL)	132
PEG-PLLA	BCNU	Encapsulation	C6 (brain cancer cell)	45–70% of sustained drug release in 10 h <i>in vitro</i>	BCNU release follows a diffusion mechanism at the early period	142
PCL, PCG-C18	SN-38 or CPT-11	Blending	HT-29 (colorectal cancer cell)	Sustained drug release for 70 days <i>in vitro</i>	The dopant PGC-C18 dramatically slowed the drug release	143
PVA/CS	DOX	Co-axial	SKOV3 (ovary cancer cell)	43–70% of sustained drug release in 120 h <i>in vitro</i>	The release rate can be adjusted by changing the ratio of core polymer to shell polymer	144
PLLA	DOX	Blended	EMT6 (breast cancer cell)	Near 50% of drug released in 10 h <i>in vitro</i>	Drug release profiles were similar between 3% and 6% Dox fibers	145

KEY: Poly(lactide-*co*-glycolide) (PLGA), paclitaxel (PTX), poly(glycerol monostearate-*co*- $\epsilon$ -caprolactone) (PGC-C18), polyvinyl alcohol (PVA), chitosan (CS), doxorubicin (DOX), temozolomide (TMZ), 1,3-bis(2-chloroethyl)-1-nitrosoures (BCNU).

affect the kinetics of ligand release. A large fiber diameter or a thick layer of packed nanofibers may allow for slow release due to inhibited water penetration and slowed diffusion of drug from relatively protected polymer strands.

To study the influence of nanofiber diameter and surface area on drug release rate, paclitaxel (PTX)-loaded PLGA fibers were fabricated with submicron ( $930 \pm 35$  nm) and micron-sized ( $3.5 \pm 0.32$   $\mu$ m) diameters.<sup>116</sup> Both fibrous platforms exhibited sustained release *in vitro* over 80 days, and higher release rates were observed with smaller-diameter fibers, attributed to their increased rate of degradation and higher relative surface area.<sup>116</sup> The *in vivo* delivery of PTX has also been investigated using similar PTX-loaded electrospun fibers of variable diameter.<sup>120</sup> Smaller diameter PTX-loaded PLGA fibers showed increased drug penetration distance through the interstitial space in a murine intracranial U87 glioma xenograft model (5 mm penetration after 42 days post-implantation), compared with lower drug penetration distance using larger submicron-sized fibers.

Construction of multilayered/stacked 3D nanofiber mats has been performed using nanofibers of alternating orientation or unidirectional layers of alternating nanofiber (or loaded drug) composition. A trilayer electrospun mesh was designed using two solvent wetting-resistant “shield” layers, surrounding a drug-loaded core layer. This design resulted in prolonged ligand release kinetics, with slow initial release over 10 days and sustained release over 30 days.<sup>139</sup> An *in vitro* cytotoxicity study was performed, in which nanofiber mats were incubated with Lewis Lung Carcinoma (LLC) cells in serum-containing media, and the trilayered mesh was loaded with antineoplastic drug SN-38. This system was shown to maintain extended cytotoxicity towards LLC cells for over 20 days.

In a separate study, four-layered polylactide nanofiber stacks were assembled with the following scheme: (i) basement mesh, (ii) drug-loaded mesh, (iii) barrier mesh, (iv) second drug-loaded mesh.<sup>140</sup> Release of drug from the second drug-loaded layer iv was observed within the first 30 min, while no detectable release of drug from the inner layer ii occurred on this timeframe. After 1 hour, release of the drug from the inner barrier-protected layer was detected. This model of timed-release multilayered constructs was implemented in a study for prevention of post-operative local cervical carcinoma recurrence, with dichloroacetate and oxaliplatin as embedded chemotherapy agents.<sup>141</sup> Using delayed dual-release nanofiber designs, synergistic multidrug combinations can be delivered, providing a new means to overcome chemoresistance encountered with use of a single drug. Additional progress is needed to scale this technology towards production for clinical use, and further investigation is needed to fully ascertain the extent of diffusion dynamics from a range of nanofiber macrostructures.

#### 4.3. Chemotherapeutic delivery

Local delivery of antineoplastic agents can, in the appropriate clinical setting, be a useful adjunct to traditional systemic chemotherapy. The Gliadel<sup>®</sup> Wafer was the first commercially available drug delivery implant approved for glioma treatment.<sup>146</sup> Gliadel is not a nanofiber material, and instead

utilizes polifeprosan 20, a synthetic biodegradable *co*-polymer (1,3-bis(*p*-carboxyphenoxy)propane and sebacic acid; 20:80 molar ratio), containing the alkylating agent carmustine (BCNU) embedded within the polymer macrostructure.<sup>147,148</sup> Clinically, Gliadel has been shown to increase survival of GBM-diagnosed patients on average by 2 months relative to those without the treatment.<sup>148,149</sup> Early drug release is a known limitation of this delivery formulation, resulting from rapid BCNU hydrolysis as well as polymer degradation.<sup>150</sup> The field of local drug delivery is anticipated to advance substantially through nanofiber-based materials, benefitting from the deformational ability of nanofibers in 3-dimensional tissue cavities, and the potential for smart nanomaterials design to allow multi-component delivery with tunable release kinetics.<sup>151</sup> BCNU-loaded poly(lactic-*co*-glycolic acid) PLGA nanofiber membranes were constructed, and these membranes could be contoured *in situ* to rest along the surface of irregular brain tissue geometry. The BCNU-PLGA system demonstrated sustained drug release of high BCNU concentrations for up to 6 weeks while avoiding significant immunogenicity.<sup>113</sup>

Yan *et al.* used coaxial electrospinning to construct polyvinyl alcohol/chitosan (PVA/CS) core-shell nanofibers, loaded with the topoisomerase II-inhibitor doxorubicin (DOX).<sup>144</sup> While lower immediate cytotoxicity was observed *in vitro* when human ovarian cancer cells (SKOV3) were exposed to DOX-loaded PVA/CS nanofibers (compared to free DOX), the PVA/CS-DOX nanofiber system was found capable of delivering drug to the tumor cell nucleus, and preventing SKOV3 cellular attachment and proliferation over a sustained duration. In a separate study, flexible drug-loaded nanofiber mats were constructed *via* electrospinning of DOX-encapsulated poly(L-lactide) (PLLA).<sup>145</sup> Mice bearing secondary hepatic carcinoma (SHCC) were treated with surgically-implanted DOX-loaded nanofiber mats adjacent to the tumor-bearing liver. Inhibited tumor growth was observed, with survival increased from 14 days (untreated) to 38 days using the new treatment. Yohe *et al.* presented a nanofiber mesh constructed from electrospun poly( $\epsilon$ -caprolactone) PCL and the polymer dopant poly(glycerol monostearate-*co*- $\epsilon$ -caprolactone) (PGC-C18).<sup>143</sup> With the use of hydrophobic PGC-C18, the authors observed an advantageous delay in aqueous diffusion through the mesh, with entrapped air serving further to prevent burst release of active drug. When the mesh was loaded with the anticancer drug SN-38, cytotoxicity in the cultured human colorectal cell line (HT-29) was seen for >90 days.<sup>143</sup> This nanofiber mesh was noted to have high mechanical strength, and authors suggested that such a mesh could potentially be incorporated as a structural reinforcement for bowel anastomosis in the setting of simultaneous cancerous bowel resection and treatment.

#### 4.4. Nanoparticle-embedded nanofibers for chemotherapy

A fundamental goal in the effective design of drug-loaded nanofibers is to avoid initial bolus/burst release of drug. Burst release is more likely to occur when using hydrophilic small-molecule compounds along with a relatively hydrophobic polymer during the electrospinning process. Probability of burst

release may also be increased if evaporation of nonpolar solvents leads to localization of the ligand primarily at the nanofiber surface.<sup>152</sup> One method of minimizing burst release involves doping of nanofibers with drug-bound nanoparticles. Nanoparticles can increase the consistency of drug release by generating an extra barrier for volatile drug diffusion *via* ionic/hydrophobic interactions between nanoparticles and drugs.<sup>153</sup> Qiu *et al.* incorporated DOX-loaded mesoporous silica nanoparticles (MSN) within PLLA nanofibers *via* electrospinning.<sup>154</sup> DOX release profiles showed a decrease in initial drug release in the nanoparticle-bearing fibers (19.2% DOX released) compared to those without nanoparticles (40% DOX released) over 60 hours *in vitro*.

Electrospun nanofiber–nanoparticle constructs may simultaneously exploit the surface chemistry of the separate constituents, with ligand elution from drug-bound nanoparticle occurring on a separate timeframe from drug release by the nanofiber. Nanoparticle and nanofiber may also bind and release separate compounds to achieve co-delivery. Chen *et al.* presented a dual-delivery system using PLGA nanofibers to deliver DOX and hydroxycamptothecin (CPT). The therapeutic agents in this case were bound to MSN and hydroxyapatite nanoparticles, incorporated within PLGA nanofibers. When tested *in vitro*, both drugs showed a sustained controlled release profile. This co-delivery method showed improved ability to inhibit growth of cervical cancer (HeLa) cells compared with single drug-loaded nanofibers.<sup>155</sup> Co-Delivery systems have the potential for synergistic therapeutic effects, which could allow the dosage of individual drugs to be decreased.

#### 4.5. Nanoparticle-embedded nanofibers for hyperthermia

Hyperthermia is a well-investigated experimental antineoplastic strategy, with tumor cells often prone to increased thermal sensitivity compared to normal tissue.<sup>156</sup> Higher temperature can render cells more susceptible to killing by approaches including chemotherapy, radiotherapy, and immunotherapy, and hyperthermia may act as a synergistic adjunct or sensitizer to the effects of concurrent drug release.<sup>157–159</sup> While magnetic nanoparticle-based inductive hyperthermia is a highly promising technique, nanoparticle delivery confronts many of the same obstacles as conventional drug delivery, including the need to sustain nanoparticle concentration at the target site, while preventing fast recognition/elimination by the reticuloendothelial and immune systems.<sup>153</sup> Magnetic nanoparticle-embedded nanofibers have been conceptualized to combine the benefits of both, and deliver the thermotherapeutic agent in a sustained manner, often in further combination with a small molecule drug.

Iron oxide nanoparticles and the antineoplastic drug bortezomib (BTZ) were incorporated into fibers constructed from copolymer poly(methyl methacrylate-*co*-dopamine methacrylamide) p(MMA-*co*-DMA).<sup>160</sup> These nanofibers provided pH-responsive drug release, while retaining iron oxide nanoparticles for sequential hyperthermia treatment. The effects of hyperthermia and chemotherapy were studied *in vitro* using human breast cancer (MCF-7) and mouse mammary carcinoma (4T1) cells, resulting in an increase in cell death (30% for MCF-



Fig. 9 Representation of tumor guide with nanofiber insert in 3D schematic rendering of the brain as well as digital top view image of extracted rat brain. Reprinted with permission from ref. 162. Copyright 2014, Springer Nature.

7 and 35% for 4T1) compared to that by hyperthermia alone (11% for MCF-7 and 29% for 4T1). Kim *et al.*<sup>161</sup> fabricated thermally-responsive nanofibers from an *N*-isopropylacrylamide (NIPAAm) and *N*-hydroxymethylacrylamide (HMAAm) *co*-polymer, along with loaded DOX and magnetic nanoparticles. An alternating magnetic field was applied to generate the thermal response, which triggered drug release from the construct. When applied to human melanoma cells (COLO 679), the combined *in vitro* effects of thermotherapy and heat-elicited drug release was 70% cell death within 5 minutes.

#### 4.6. Dual migration and drug delivery platforms

Novel platforms can be designed to utilize the potential of nanofibers for drug delivery and simultaneously influence patterns of tumor cell migration. In a study by Jain *et al.*, implanted nanofibers functioned as a treatment modality *via* their effects on cell migration alone (Fig. 9).<sup>162</sup> A PCL-based nanofiber “tumor guide” was used to promote migration of U87 glioblastoma cells away from an intracortical tumor and toward an extracortical scaffold. Once cells were located outside the brain, the cyclopamine-conjugated hydrogel in the scaffold triggered tumor cell apoptosis. The result of this approach was to decrease bulk tumor volume along with the visualized extent of perilesional tumor cell invasion. Relative to a smooth film surface, F-actin staining of cells in the tumor conduit confirmed a migratory cell phenotype that was enhanced when the conduit used aligned nanofibers. This study supported the potential of tumor relocation by presenting cells a preferential and topographically directed migration pathway.

## 5. Nanofibers for circulating tumor cell filtration and detection

### 5.1 Circulating tumor cell filtration

Identification of circulating tumor cells (CTCs) is an active area of research, with potential for cancer diagnosis and monitoring through less-invasive means. Circulating tumor cells (CTCs) can persist transiently within fluid compartments (*e.g.* blood, CSF, peritoneal fluid, accumulated interstitial fluid) that are available for sampling, independent of the primary tumor.<sup>163,164</sup> Circulating cells may function as biomarkers for early detection of solid

tumors or hematologic malignancies.<sup>165–167</sup> Increased concentration of CTCs has proven predictive of tumor progression as well as reduced overall survival in breast,<sup>168–170</sup> prostate,<sup>170,171</sup> colorectal,<sup>170,172</sup> gastric,<sup>173</sup> and lung cancer.<sup>174</sup> In metastatic breast cancer, 5 or more CTCs in 7.5 mL of blood has been shown to correlate with poor prognosis.<sup>163</sup> Prostate cancer CTCs have been found to contain the same genetic alterations as the primary tumor<sup>175</sup> and were more accurately predictive of overall survival compared to measurement of prostate-specific antigen (PSA).<sup>165,171</sup> In small cell lung cancer, CTCs were found to recapitulate the primary tumor biology when cultured.<sup>30</sup> Fluid sampling has relatively lesser morbidity, low technical difficulty, and can offer the option of repeat sampling. By comparing multiple samples over time, CTC characteristics such as mobility, presence of surface proteins for cellular adhesion, and markers of epithelial to mesenchymal transition provide even more data to evaluate clinical disease progression.

Current methods of CTC capture are based on either physical property differences (label-independent) or immunoaffinity differences (label-dependent) between CTCs and blood cells. Since CTCs are normally larger and stiffer than blood cells, a filtering microchip can be used for filtering CTCs.<sup>176</sup> However, the problem with the specificity of CTC isolation and clogging on the filtering device been reported in this type of application. The recognition of a specific protein marker on the tumor cell surface by an antibody allows for the development of label-dependent devices.<sup>30,177–179</sup> During positive selection, tumor-associated cell surface antigens (*e.g.* epithelial cell adhesion molecule; EpCAM) are targeted. Processes of negative selection are also used to actively exclude background cells with antigens not expressed on CTCs (*e.g.* leukocyte common antigen; CD45). In addition, physical differences between CTCs and surrounding cells (size, shape density, deformability, and electrical characteristics) may be incorporated in CTC capture.<sup>180–182</sup>

Both the wide variation of compounds present in biological samples and the low number (0.00004%) of cells disseminated from the primary tumor that metastasize represent barriers to optimization of capture technique.<sup>61,183,184</sup> Advances in capture techniques require improved ability to filter single cells while retaining the cells' biological characteristics. Nanofibers have shown promise in this arena, as the nanoscale fibrous structure can be designed to mimic native microenvironment topography, with dimensional attributes and surface ligands familiar to the cellular population of interest.<sup>185</sup> A favorable 3-D environment both facilitates target cell attachment and helps to maintain native tumor cell behavior between capture and subsequent culture stages.

Zhang *et al.*<sup>186</sup> demonstrated the benefits of the nanofiber topography for CTC capture when comparing anti-EpCAM grafted TiO<sub>2</sub> nanofibers (100–300 nm diameter) with a flat antigen-bound silicon substrate. Cells became adherent to the nanofiber surface and fully extended pseudopodia, indicating appropriate affinity to the substrate. Yang *et al.*<sup>187</sup> investigated the combined effect of nanofiber topography and chemical cues on cellular attachment. Polydopamine (PDA) nanoparticles were incorporated to form pendants within the nanofiber structure

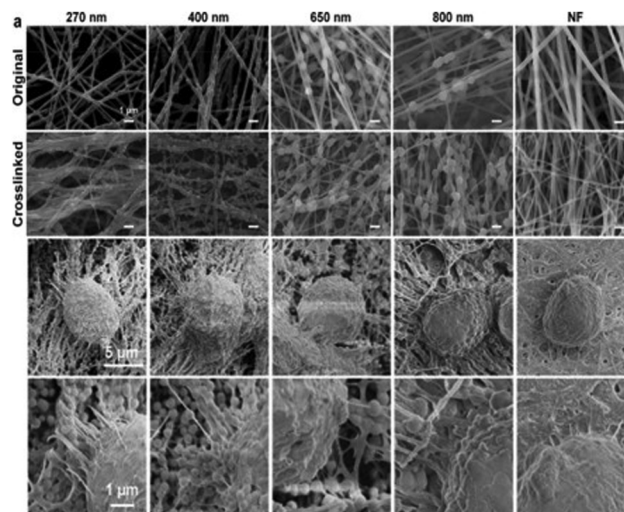


Fig. 10 SEM images of pendant polydopamine (PDA) nanoparticle-alginate nanofibers, with PDA diameters ranging from 270–800 nm and nanofibers without PDA (NF); top two image panels show nanofibers before and after alginate crosslinking. Bottom two image panels show PDA-alginate nanofibers cultured with human pancreatic carcinoma cells (PANC-1). Reprinted with permission from ref. 187. Copyright 2018, American Chemical Society.

that were seen to facilitate cellular adhesion, potentially related to an increase in topographical complexity (Fig. 10).

Focusing on improvements in downstream CTC analysis, Liu *et al.*<sup>188</sup> described a microfluidic device for CTC capture and release, using anti-EpCAM-conjugated MnO<sub>2</sub> electrospun nanofibers (400–800 nm) coated within a polydimethylsiloxane (PDMS) microfluidic channel. Inlet and outlet were created in the PDMS serpentine fluid layer for sample solution to pass through the microfluidic channel. Release of cells was induced through oxalate dissolution of MnO<sub>2</sub> nanofibers, with an 88% cell release rate observed. The authors noted an increase in cell capture efficiency with increased nanofiber density, concluding that local topography and nanofiber packing were effective methods to alter cell adhesion. Similarly, microfluidic chips that were embedded with random or aligned electrospun PLGA nanofibers were fabricated by Yu *et al.*<sup>189</sup> The PLGA nanofiber array-coated glass cover slip (bottom) was bonded with a PMMA top plate where two holes were drilled as the inlet and outlet of the microfluidic chip. 80.5% of cell capture yield was achieved in the optimal conditions. The captured cells were released by continuous injection of air foam into the microfluidic devices. Interestingly, the random nanofiber device was found to have higher capture efficiency and cell recovery rate than the aligned nanofiber device. Zhao *et al.*<sup>190</sup> integrated anti-EPCAM-loaded PLGA nanofibers with a microfluidic chip-based cell capture design, and used laser capture microdissection (LCM) to interact with immobilized cells. The authors reported a capture efficiency of 74.7% from blood samples bearing prostate cancer CTCs. LCM was able to successfully extract and sequence CTCs using Exome-Seq.<sup>190</sup> Additional work with this microfluidic chip-based nanofiber CTC platform was reported by Hou *et al.*<sup>191</sup> Using a melanoma-specific biotinylated anti-CD146

surface for capture, an 87% capture efficiency was demonstrated with melanoma cells (M229). Post-capture immunocytochemical analysis of four biomarkers resulted in the detection of approximately 40 CTCs per sample. Cells were then extracted by laser microdissection for further sequencing, resulting in the detection of the BRAFV600E mutation. This mutation detected from CTCs matched molecular genomic analysis from the original tumor biopsy. Electrospun nanofiber-integrated CTC systems represent a promising methodology for further advances in indirect tumor diagnosis and disease monitoring.<sup>192–194</sup>

## 5.2 Cancer detection

In addition to direct capture of CTC, cancer detection *via* sensing of cancer-associated factors and genes has also been widely investigated for cancer diagnosis and oncology research. Due to the advantages of high surface-to-volume ratio and porous structure, electrospun nanofiber-based sensors provide higher specificity and sensitivity than conventional solid film-based sensor.<sup>195</sup> Fig. 11 illustrates several examples of cancer detection applications.

Hypoxia, an oxygen deficiency condition, is generally found in solid tumors due to the imbalance between uncontrollable tumor growth and short oxygen supply by tumor blood vessels.<sup>196</sup> The low oxygen concentration is regarded as an indicator of cancer cell and thus can be characterized locally by a nanofiber-based oxygen sensor. A biocompatible nanofiber sensor was developed by Xue *et al.* that allows for locating and imaging of hypoxic regions below cultured glioblastoma cell line aggregates.<sup>197</sup> The fibers were co-axially electrospun and consist of a biocompatible PCL shell and a gas-permeable polycarbonate (PC) core. An oxygen sensitive luminescence probe, Pd(II) *meso*-tetra(pentafluorophenyl) porphine (PdTFPP),

was embedded within the core material and can provide micro-scale oxygen sensing. Compared to most reported film-based optical oxygen sensors, an electrospun nanofiber based sensor is ECM-mimicking and thus offer more accurate identification of localized oxygen conditions and cancer detection.

Elevated levels of reactive oxygen species (ROS) have been shown in cancer cells compared to noncancerous cells. Detection of ROS, such as hydrogen peroxide (H<sub>2</sub>O<sub>2</sub>), holds promise for cancer diagnosis. For instance, Zhang *et al.* designed an electrospun bimetallic Au–Ag/Co<sub>3</sub>O<sub>4</sub> nanofiber sensor for sensitive detection of hydrogen peroxide released from human breast cancer cells.<sup>198</sup> Leveraging the advantage of large surface-to-volume ratio, the Au–Ag/Co<sub>3</sub>O<sub>4</sub> nanofibers served as efficient electrocatalysts for oxidation of H<sub>2</sub>O<sub>2</sub> and demonstrated a high detection sensitivity towards H<sub>2</sub>O<sub>2</sub>. Other types of sensors for the detection of H<sub>2</sub>O<sub>2</sub> have also been investigated and reviewed, including spectrophotometry-, chromatography- and chemiluminescence-based sensors.<sup>195</sup>

Tumor-associated genes, such as p53 gene, are biological markers of cancer development. Wang and his collaborators developed an electrochemical p53 biosensor comprising of carboxylated multi-walled carbon nanotubes (MWNTs) nylon 6 (PA6) composite nanofibers (MWNTs–PA6) by electrospinning.<sup>199</sup> Single-stranded DNA (ssDNA) was immobilized on electrospun nanofibers and can hybridize with wild type p53 sequences, which can be detected by an electrochemical indicator methylene blue (MB). With large specific surface area and good biocompatibility, the sensor can detect 50 femtomolar wild type p53 sequence. This design opens up the possibilities for other tumor-associated gene detection.

## 6. Conclusions and future outlook

Scientific progress in polymer chemistry and technological advancement in electrospinning have enabled the production of nanofibers that serve as multi-functional constructs for cancer research and treatment. Polymeric nanofiber matrices can be electrospun with the objective of generating architectural similarity to the native tumor microenvironment. Nanofiber systems can serve as reproducible models for cancer research and preclinical cancer treatment screening. Owing to straightforward drug incorporation during the electrospinning process, large nanofiber surface area to volume ratio, porous architecture, and tunable material properties, nanofibers can function as controllable delivery platforms for sustained drug release. This application has been further expanded by the use of more complex multi-component nanofiber designs, as well as dual nanoparticle-nanofiber systems. Nanofibers can also be engineered to capture circulating tumor cells and cancer biomarkers, promote cell attachment and maintain native biological cell behaviors. The small number of circulating cancer cells and biomarkers present within a large volume of complex biological fluid requires (1) ultrahigh sensitivity/specificity for nanofiber sensors and (2) meticulous design/testing of the sensors.

Despite significant advances in recent years, barriers remain for clinical translation of novel nanofiber structures in the field



**Fig. 11** Cancer detection by electrospun nanofibers. (a) Schematic illustration of nanofiber-based detection of oxygen, gene, and ROS. (b) U251 glioblastoma cells (green) adhered to fibers in hypoxia (1% O<sub>2</sub>) or normoxic (21% O<sub>2</sub>) conditions detected by nanofibers. Reprinted with permission from ref. 197. Copyright 2016, Elsevier. (c) Schematic diagram of Au–Ag/Co<sub>3</sub>O<sub>4</sub> nanofibers used for detection of H<sub>2</sub>O<sub>2</sub> efflux from MCF-7 stimulated by phorbol 12-myristate 13-acetate (PMA) (left) and detection signals (amperometric responses) obtained at the Au–Ag/Co<sub>3</sub>O<sub>4</sub>NFS/GCE in the absence and presence of MCF-7 with the addition of pma and catalase (right). Reprinted with permission from ref. 198. Copyright 2018, Elsevier. (d) Schematic diagram of an electrochemical p53 biosensor comprising of carboxylated multi-walled carbon nanotubes (MWNTs) and nylon 6 (PA6) composite nanofibers (MWNTs–PA6) by electrospinning. Reprinted with permission from ref. 199. Copyright 2013, Elsevier.

of cancer research and therapeutics. Our scientific understanding continues to evolve regarding cancer cell response to topographical, physical and biochemical cues. The impact of electrospun fibers on cell proliferation, attachment, migration, morphology, signalling, and expression of biomarkers must be fully assessed to produce an optimized biomimetic ECM for cancer drug screening. Most of the reviewed nanofibers in 3D scaffolds are aligned randomly, parallelly, or orthogonally in two dimensions due to the limit of electrospinning technique. Hierarchical complexity of tumor ECM presents a significant challenge for biomimetic design, and further investigation is required to precisely and reproducibly control the morphology of deposited fibers at the nanoscale. Achieving this goal requires knowledge of the key targeted ECM parameters that promote an invasive tumor phenotype and best methods of nanofiber synthesis to match the required ECM morphology.

Drug loading in nanofibers must overcome challenges of uneven drug distribution. Variably distributed drug within the nanofiber construct can contribute to disadvantageous burst release from areas of high drug loading.<sup>200</sup> Information of total drug dosage in most reported nanofibers is obscure. Difficulties remain in loading a high drug dosage into nanofibers that satisfy the requirement in clinical studies in humans.<sup>201</sup> Accordingly, the *in vivo* drug release profile of nanofibers, including drug release kinetics and dynamics, bio-distribution, dosage, and cytotoxicity needs to be carefully examined before clinical translation. In addition to their role as a drug loading platform for chemotherapy, nanofibers have the potential to augment the therapeutic effects of other treatments such as radiotherapy and immunotherapy. Augmented immunotherapy might be achieved on implanted nanofibers conjugated with immunomodulatory cytokines, benefiting from preferential adhesion and migration of cancer cells on nanofibers.

The commercialization of nanofiber-based sensors remains in its infancy, as evidenced by few successful products that are currently available. CTCs with heterogeneous phenotypes and markers should be evaluated in their entirety for the more wide-ranging CTC capture and detection. Issues of uniform fiber size and composition are further complicated when considering the translation to industrial manufacturing scale. From this perspective, fabrication costs and long-term stability of the sensors need to be addressed before commercialization.

Overall, technical and systematic challenges exist for the widespread implementation and utilization of electrospun nanofibers in the field of oncology. Collaborative efforts from clinicians, chemists, biologists, and material scientists are imperative for the appropriate translation of novel technologies based on electrospun nanofibers. As the understanding of cellular and molecular interactions within electrospun nanofibers continues to advance, it is expected that this research area will present practical opportunities to appropriately address significant clinical needs within the areas of 3-D tumor modelling, anti-neoplastic drug delivery, and cancer diagnostics.

## Conflicts of interest

There are no conflicts to declare.

## Acknowledgements

This work is supported in part by Kyocera Professor Endowment to M. Z. A. E. E. acknowledges support from the National Science Foundation Graduate Research Fellowship Program. S. L. L. acknowledges support from the Ruth L. Kirschstein NIH Training grant T32CA138312. P. A. C. acknowledges Children's Cancer Research Fund, the Otis Booth Foundation, the Wright Foundation, as well as generous philanthropic support.

## References

- 1 R. L. Siegel, K. D. Miller, H. E. Fuchs and A. Jemal, Cancer statistics, *CA-Cancer J. Clin.*, 2022, **72**, 7–33.
- 2 D. Hanahan and R. A. Weinberg, Hallmarks of Cancer: The Next Generation, *Cell*, 2011, **144**, 646–674.
- 3 D. Hanahan and R. A. Weinberg, The Hallmarks of Cancer, *Cell*, 2000, **100**, 57–70.
- 4 D. Miller Kimberly, *et al.*, Cancer treatment and survivorship statistics, 2016, *CA-Cancer J. Clin.*, 2016, **66**, 271–289.
- 5 J. Jeevanandam, A. Barhoum, Y. S. Chan, A. Dufresne and M. K. Danquah, Review on nanoparticles and nanostructured materials: history, sources, toxicity and regulations, *Beilstein J. Nanotechnol.*, 2018, **9**, 1050–1074.
- 6 X. Q. Liu and R. Z. Tang, Biological responses to nanomaterials: understanding nano-bio effects on cell behaviors, *Drug Delivery*, 2017, **24**, 1–15.
- 7 P. A. Chiarelli, F. M. Kievit, M. Zhang and R. G. Ellenbogen, Bionanotechnology and the future of glioma, *Surg. Neurol. Int.*, 2015, **6**, S45–S58.
- 8 M. Keshvaridoostchokami, *et al.*, Electrospun Nanofibers of Natural and Synthetic Polymers as Artificial Extracellular Matrix for Tissue Engineering, *Nanomater. Basel Switz.*, 2020, **11**, 21.
- 9 S. Ramakrishna, *et al.*, Electrospun nanofibers: solving global issues, *Mater. Today*, 2006, **9**, 40–50.
- 10 W. E. Teo and S. Ramakrishna, A review on electrospinning design and nanofibre assemblies, *Nanotechnology*, 2006, **17**, R89–R106.
- 11 X. Hu, *et al.*, Electrospinning of polymeric nanofibers for drug delivery applications, *J. Controlled Release*, 2014, **185**, 12–21.
- 12 S. Kajdič, O. Planinšek, M. Gašperlin and P. Kocbek, Electrospun nanofibers for customized drug-delivery systems, *J. Drug Delivery Sci. Technol.*, 2019, **51**, 672–681.
- 13 A. Akhgari, Z. Shakib and S. Sanati, A review on electrospun nanofibers for oral drug delivery, *Nanomed. J.*, 2017, **4**, 197–207.
- 14 R. Malik, T. Garg, A. K. Goyal and G. Rath, Polymeric nanofibers: targeted gastro-retentive drug delivery systems, *J. Drug Target*, 2015, **23**, 109–124.
- 15 M. Cavo, *et al.*, Electrospun nanofibers in cancer research: from engineering of *in vitro* 3D cancer models to therapy, *Biomater. Sci.*, 2020, **8**, 4887–4905.
- 16 J. Li, Y. Liu and H. E. Abdelhakim, Drug Delivery Applications of Coaxial Electrospun Nanofibres in Cancer Therapy, *Molecules*, 2022, **27**, 1803.

- 17 E. Jagtiani and A. S. Sabnis, Recent advancements of electrospun nanofibers for cancer therapy, *Polym. Bull.*, 2022, **1**–28.
- 18 N. H. A. Tran, H. Brünig, M. A. der Landwehr and G. Heinrich, Controlling micro- and nanofibrillar morphology of polymer blends in low-speed melt spinning process. Part III: fibrillation mechanism of PLA/PVA blends along the spinline, *J. Appl. Polym. Sci.*, 2016, **133**, 44259.
- 19 M. Kamiyama, T. Soeda, S. Nagajima and K. Tanaka, Development and application of high-strength polyester nanofibers, *Polym. J.*, 2012, **44**, 987–994.
- 20 A. Suzuki, K. Hosoi and K. Miyagi, Broad poly(ethylene terephthalate) nanofiber sheet prepared by CO<sub>2</sub> laser supersonic continuous multi-drawing, *Polymer*, 2015, **60**, 252–259.
- 21 S. Zhong, Y. Zhang and C. T. Lim, Fabrication of Large Pores in Electrospun Nanofibrous Scaffolds for Cellular Infiltration: A Review, *Tissue Eng., Part B*, 2011, **18**, 77–87.
- 22 H. M. Estabridis, A. Jana, A. Nain and D. J. Odde, Cell Migration in 1D and 2D Nanofiber Microenvironments, *Ann. Biomed. Eng.*, 2018, **46**, 392–403.
- 23 A. S. Nain, *et al.*, Control of Cell Behavior by Aligned Micro/Nanofibrous Biomaterial Scaffolds Fabricated by Spinneret-Based Tunable Engineered Parameters (STEP) Technique, *Small*, 2008, **4**, 1153–1159.
- 24 P. Sharma, *et al.*, Aligned and suspended fiber force probes for drug testing at single cell resolution, *Biofabrication*, 2014, **6**, 045006.
- 25 B. Raghavan, H. Soto and K. Lozano, Fabrication of Melt Spun Polypropylene Nanofibers by Forcespinning, *J. Eng. Fibers Fabr.*, 2013, **8**, 155892501300800100.
- 26 K. Sarkar, *et al.*, Electrospinning to Forcespinning<sup>TM</sup>, *Mater. Today*, 2010, **13**, 12–14.
- 27 A. E. Erickson, *et al.*, High-Throughput and High-Yield Fabrication of Uniaxially-Aligned Chitosan-Based Nanofibers by Centrifugal Electrospinning, *Carbohydr. Polym.*, 2015, **134**, 467–474.
- 28 D. Wouters and U. S. Schubert, Nanolithography and Nanochemistry: Probe-Related Patterning Techniques and Chemical Modification for Nanometer-Sized Devices, *Angew. Chem., Int. Ed.*, 2004, **43**, 2480–2495.
- 29 A. A. Tseng, A. Notargiacomo and T. P. Chen, Nanofabrication by scanning probe microscope lithography: a review, *J. Vac. Sci. Technol., B: Microelectron. Nanometer Struct. – Process., Meas., Phenom.*, 2005, **23**, 877–894.
- 30 C. L. Hodgkinson, *et al.*, Tumorigenicity and genetic profiling of circulating tumor cells in small-cell lung cancer, *Nat. Med.*, 2014, **20**, 897–903.
- 31 D. Li and Y. Xia, Electrospinning of Nanofibers: Reinventing the Wheel?, *Adv. Mater.*, 2004, **16**, 1151–1170.
- 32 Y. Wan, Z. Yang, G. Xiong, S. R. Raman and H. Luo, Bacterial cellulose-templated synthesis of free-standing silica nanotubes with a three-dimensional network structure, *RSC Adv.*, 2015, **5**, 48875–48880.
- 33 D. Liang, B. S. Hsiao and B. Chu, Functional electrospun nanofibrous scaffolds for biomedical applications, *Adv. Drug Delivery Rev.*, 2007, **59**, 1392–1412.
- 34 H. Zhang, X. Liu, M. Yang and L. Zhu, Silk fibroin/sodium alginate composite nano-fibrous scaffold prepared through thermally induced phase-separation (TIPS) method for biomedical applications, *Mater. Sci. Eng., C*, 2015, **55**, 8–13.
- 35 J. M. D'Arcy, *et al.*, Vapor-Phase Polymerization of Nanofibrillar Poly(3,4-ethylenedioxythiophene) for Supercapacitors, *ACS Nano*, 2014, **8**, 1500–1510.
- 36 Y. Wan, *et al.*, Directional fluid induced self-assembly of oriented bacterial cellulose nanofibers for potential biomimetic tissue engineering scaffolds, *Mater. Chem. Phys.*, 2015, **149–150**, 7–11.
- 37 M. R. Williamson and A. G. A. Coombes, Gravity spinning of polycaprolactone fibres for applications in tissue engineering, *Biomaterials*, 2004, **25**, 459–465.
- 38 N. P. Truong, J. F. Quinn, M. R. Whittaker and T. P. Davis, Polymeric filomicelles and nanoworms: two decades of synthesis and application, *Polym. Chem.*, 2016, **7**, 4295–4312.
- 39 G. I. Taylor and M. D. Van Dyke, Electrically driven jets, *Proc. R. Soc. London, Ser. A*, 1969, **313**, 453–475.
- 40 A. L. Yarin, S. Koombhongse and D. H. Reneker, Bending instability in electrospinning of nanofibers, *J. Appl. Phys.*, 2001, **89**, 3018–3026.
- 41 D. H. Reneker and A. L. Yarin, Electrospinning jets and polymer nanofibers, *Polymer*, 2008, **49**, 2387–2425.
- 42 O. O. Dosunmu, G. G. Chase, W. Kataphinan and D. H. Reneker, Electrospinning of polymer nanofibres from multiple jets on a porous tubular surface, *Nanotechnology*, 2006, **17**, 1123–1127.
- 43 A. L. Yarin and E. Zussman, Upward needleless electrospinning of multiple nanofibers, *Polymer*, 2004, **45**, 2977–2980.
- 44 A. K. Moghe and P. B. S. Gupta, Co-axial Electrospinning for Nanofiber Structures: Preparation and Applications, *Polym. Rev.*, 2008, **48**, 353–377.
- 45 X. Wang, *et al.*, Formation of water-resistant hyaluronic acid nanofibers by blowing-assisted electro-spinning and non-toxic post treatments, *Polymer*, 2005, **46**, 4853–4867.
- 46 I. C. Um, D. Fang, B. S. Hsiao, A. Okamoto and B. Chu, Electro-spinning and electro-blowing of hyaluronic acid, *Biomacromolecules*, 2004, **5**, 1428–1436.
- 47 Y. Lin, *et al.*, Preparation of poly(ether sulfone) nanofibers by gas-jet/electrospinning, *J. Appl. Polym. Sci.*, 2008, **107**, 909–917.
- 48 A. Khalil, R. Hashaikeh and M. Jouiad, Synthesis and morphology analysis of electrospun copper nanowires, *J. Mater. Sci.*, 2014, **49**, 3052–3065.
- 49 W.-E. Teo, R. Inai and S. Ramakrishna, Technological advances in electrospinning of nanofibers, *Sci. Technol. Adv. Mater.*, 2011, **12**, 013002.
- 50 N. M. Thoppey, J. R. Bochinski, L. I. Clarke and R. E. Gorga, Edge electrospinning for high throughput production of quality nanofibers, *Nanotechnology*, 2011, **22**, 345301.
- 51 T. Lei, Z. Xu, X. Cai, L. Xu and D. Sun, New Insight into Gap Electrospinning: Toward Meter-long Aligned Nanofibers, *Langmuir*, 2018, **34**, 13788–13793.

- 52 Z. Jianrui, Y. Yurong and L. Shicheng, Research progress in collector and auxiliary electrode for electrospinning process, *China Synth. Fiber Ind.*, 2009, **15**(5), 40–43.
- 53 L. Huang, *et al.*, Porous carbon nanofibers formed in situ by electrospinning with a volatile solvent additive into an ice water bath for lithium–sulfur batteries, *RSC Adv.*, 2015, **5**, 23749–23757.
- 54 P. Katta, M. Alessandro, R. D. Ramsier and G. G. Chase, Continuous Electrospinning of Aligned Polymer Nanofibers onto a Wire Drum Collector, *Nano Lett.*, 2004, **4**, 2215–2218.
- 55 J. Xue, T. Wu, Y. Dai and Y. Xia, Electrospinning and Electrospun Nanofibers: Methods, Materials, and Applications, *Chem. Rev.*, 2019, **119**, 5298–5415.
- 56 M. A. Alfaro De Prá, R. M. Ribeiro-do-Valle, M. Maraschin and B. Veleirinho, Effect of collector design on the morphological properties of polycaprolactone electrospun fibers, *Mater. Lett.*, 2017, **193**, 154–157.
- 57 M. Richard-Lacroix and C. Pellerin, Molecular Orientation in Electrospun Fibers: From Mats to Single Fibers, *Macromolecules*, 2013, **46**, 9473–9493.
- 58 S. S. Ojha, M. Afshari, R. Kotek and R. E. Gorga, Morphology of electrospun nylon-6 nanofibers as a function of molecular weight and processing parameters, *J. Appl. Polym. Sci.*, 2008, **108**, 308–319.
- 59 H. Dou, H. Liu, F. Wang and Y. Sun, Preparation and Characterization of Electrospun Polylactic Acid Micro/Nanofibers under Different Solvent Conditions, *Fluid Dyn. Mater. Process*, 2021, **17**(3), 629–638.
- 60 H. Mills, *et al.*, Preparation of PCL Electrospun Fibers Loaded with Cisplatin and Their Potential Application for the Treatment of Prostate Cancer, *Emerg. Med. Int.*, 2022, **2022**, 6449607.
- 61 Z. Chen, *et al.*, Electrospun nanofibers for cancer diagnosis and therapy, *Biomater. Sci.*, 2016, **4**, 922–932.
- 62 L. Deng, R. J. Young, I. A. Kinloch, Y. Zhu and S. J. Eichhorn, Carbon nanofibres produced from electrospun cellulose nanofibres, *Carbon*, 2013, **58**, 66–75.
- 63 D. Li and Y. Xia, Fabrication of Titania Nanofibers by Electrospinning, *Nano Lett.*, 2003, **3**, 555–560.
- 64 J. Rnjak-Kovacina and A. S. Weiss, Increasing the Pore Size of Electrospun Scaffolds, *Tissue Eng., Part B*, 2011, **17**, 365–372.
- 65 A. Izadyari Aghmiuni, S. Heidari Keshel, F. Sefat and A. AkbarzadehKhiyavi, Fabrication of 3D hybrid scaffold by combination technique of electrospinning-like and freeze-drying to create mechanotransduction signals and mimic extracellular matrix function of skin, *Mater. Sci. Eng., C*, 2021, **120**, 111752.
- 66 Y. Chen, *et al.*, Gas foaming of electrospun poly(L-lactide-co-caprolactone)/silk fibroin nanofiber scaffolds to promote cellular infiltration and tissue regeneration, *Colloids Surf., B*, 2021, **201**, 111637.
- 67 L. D. Wright, T. Andric and J. W. Freeman, Utilizing NaCl to increase the porosity of electrospun materials, *Nov. Struct. Tissue Eng.*, 2011, **31**, 30–36.
- 68 S. An, M. W. Lee, H. S. Jo, S. S. Al-Deyab and S. S. Yoon, Weaving nanofibers by altering counter-electrode electrostatic signals, *J. Aerosol. Sci.*, 2016, **95**, 67–72.
- 69 L. Fu, J. Xie, M. A. Carlson and D. A. Reilly, Three-dimensional nanofiber scaffolds with arrayed holes for engineering skin tissue constructs, *MRS Commun.*, 2017, **7**, 361–366.
- 70 B. L.-P. Lee, *et al.*, Femtosecond laser ablation enhances cell infiltration into three-dimensional electrospun scaffolds, *Acta Biomater.*, 2012, **8**, 2648–2658.
- 71 A. Eatemadi, H. Daraee, N. Zarghami, H. Melat Yar and A. Akbarzadeh, Nanofiber: synthesis and biomedical applications, *Artif. Cells, Nanomed., Biotechnol.*, 2016, **44**, 111–121.
- 72 T. J. Sill and H. A. von Recum, Electrospinning: applications in drug delivery and tissue engineering, *Biomaterials*, 2008, **29**, 1989–2006.
- 73 S. H. Park, T. G. Kim, H. C. Kim, D.-Y. Yang and T. G. Park, Development of dual scale scaffolds via direct polymer melt deposition and electrospinning for applications in tissue regeneration, *Acta Biomater.*, 2008, **4**, 1198–1207.
- 74 D. Yu, J. Wang, K. Qian, J. Yu and H. Zhu, Effects of nanofibers on mesenchymal stem cells: environmental factors affecting cell adhesion and osteogenic differentiation and their mechanisms, *J. Zhejiang Univ., Sci., B*, 2020, **21**, 871–884.
- 75 Y. Guo, J. Gilbert-Honick, S. M. Somers, H.-Q. Mao and W. L. Grayson, Modified cell-electrospinning for 3D myogenesis of C<sub>2</sub>C<sub>12</sub>S in aligned fibrin microfiber bundles, *Biochem. Biophys. Res. Commun.*, 2019, **516**, 558–564.
- 76 S. N. Jayasinghe, Cell electrospinning: a novel tool for functionalising fibres, scaffolds and membranes with living cells and other advanced materials for regenerative biology and medicine, *The Analyst*, 2013, **138**, 2215–2223.
- 77 H. S. Yoo, T. G. Kim and T. G. Park, Surface-functionalized electrospun nanofibers for tissue engineering and drug delivery, *Adv. Drug Delivery Rev.*, 2009, **61**, 1033–1042.
- 78 W. Cui, Y. Zhou and J. Chang, Electrospun nanofibrous materials for tissue engineering and drug delivery, *Sci. Technol. Adv. Mater.*, 2010, **11**, 014108.
- 79 F. Ignatious, L. Sun, C.-P. Lee and J. Baldoni, Electrospun Nanofibers in Oral Drug Delivery, *Pharm. Res.*, 2010, **27**, 576–588.
- 80 S. L. Levensgood, A. E. Erickson, F. Chang and M. Zhang, Chitosan–poly(caprolactone) nanofibers for skin repair, *J. Mater. Chem. B*, 2017, **5**, 1822–1833.
- 81 X. Wang, B. Ding and B. Li, Biomimetic electrospun nanofibrous structures for tissue engineering, *Mater. Today*, 2013, **16**, 229–241.
- 82 P. Zahedi, I. Rezaeian, S.-O. Ranaei-Siadat, S.-H. Jafari and P. Supaphol, A review on wound dressings with an emphasis on electrospun nanofibrous polymeric bandages, *Polym. Adv. Technol.*, 2010, **21**, 77–95.
- 83 Q. Guo, *et al.*, Supercapacitors based on hybrid carbon nanofibers containing multiwalled carbon nanotubes, *J. Mater. Chem.*, 2009, **19**, 2810–2816.



- 84 P. Hiralal, *et al.*, Nanomaterial-Enhanced All-Solid Flexible Zinc-Carbon Batteries, *ACS Nano*, 2010, **4**, 2730–2734.
- 85 A. Ghorbani-Choghamarani, Z. Taherinia, Z. Heidarnezhad and Z. Moradi, Application of Nanofibers Based on Natural Materials as Catalyst in Organic Reactions, *J. Ind. Eng. Chem.*, 2021, **94**, 1–61.
- 86 R. Balamurugan, S. Sundarrajan and S. Ramakrishna, Recent Trends in Nanofibrous Membranes and Their Suitability for Air and Water Filtrations, *Membranes*, 2011, **1**, 232–248.
- 87 S. Zhang *et al.*, in *Electrospun Nanofibers for Air Filtration. in Electrospinning: Nanofabrication and Applications* ed. Ding, B., Wang, X. and Yu, J., William Andrew Publishing, 2019, Chapter 12, pp. 365–389, DOI: [10.1016/B978-0-323-51270-1.00012-1](https://doi.org/10.1016/B978-0-323-51270-1.00012-1).
- 88 M. J. Bissell, D. C. Radisky, A. Rizki, V. M. Weaver and O. W. Petersen, The organizing principle: microenvironmental influences in the normal and malignant breast, *Differ. Res. Biol. Divers*, 2002, **70**, 537–546.
- 89 D. M. Noonan, G. Pennesi and A. Albin, Invasion and Metastasis. in *The Tumor Microenvironment*, ed. Bagley, R. G., Springer, 2010, pp. 213–228, DOI: [10.1007/978-1-4419-6615-5\\_10](https://doi.org/10.1007/978-1-4419-6615-5_10).
- 90 S. A. Langhans, Three-Dimensional in Vitro Cell Culture Models in Drug Discovery and Drug Repositioning, *Front. Pharmacol.*, 2018, **9**, 6.
- 91 J. C. Fontoura, *et al.*, Comparison of 2D and 3D cell culture models for cell growth, gene expression and drug resistance, *Mater. Sci. Eng., C*, 2020, **107**, 110264.
- 92 S. O. Suzuki and T. Iwaki, Dynamic analysis of glioma cells: looking into ‘movement phenotypes’, *Neuropathology*, 2005, **25**, 254–262.
- 93 Z. Liu and G. Vunjak-Novakovic, Modeling tumor microenvironments using custom-designed biomaterial scaffolds, *Curr. Opin. Chem. Eng.*, 2016, **11**, 94–105.
- 94 J. Johnson, *et al.*, Quantitative Analysis of Complex Glioma Cell Migration on Electrospun Polycaprolactone Using Time-Lapse Microscopy, *Tissue Eng., Part C*, 2009, **15**, 531–540.
- 95 F. M. Kievit, *et al.*, Aligned Chitosan-Polycaprolactone Polyblend Nanofibers Promote the Migration of Glioblastoma Cells, *Adv. Healthcare Mater.*, 2013, **2**, 1651–1659.
- 96 S. Chen, S. K. Boda, S. K. Batra, X. Li and J. Xie, Emerging Roles of Electrospun Nanofibers in Cancer Research, *Adv. Healthcare Mater.*, 2018, **7**, 1701024.
- 97 N. J. Mickevicius, *et al.*, Location of brain tumor intersecting white matter tracts predicts patient prognosis, *J. Neurooncol.*, 2015, **125**, 393–400.
- 98 C. Beadle, *et al.*, The Role of Myosin II in Glioma Invasion of the Brain, *Mol. Biol. Cell*, 2008, **19**, 3357–3368.
- 99 A. Giese and M. Westphal, Glioma invasion in the central nervous system, *Neurosurgery*, 1996, **39**, 235–250; discussion 250–2.
- 100 M. W. Conklin, *et al.*, Aligned collagen is a prognostic signature for survival in human breast carcinoma, *Am. J. Pathol.*, 2011, **178**, 1221–1232.
- 101 E. Cukierman, R. Pankov, D. R. Stevens and K. M. Yamada, Taking Cell-Matrix Adhesions to the Third Dimension, *Science*, 2001, **294**, 1708–1712.
- 102 A. Rape, B. Ananthanarayanan and S. Kumar, Engineering strategies to mimic the glioblastoma microenvironment, *Adv. Drug Delivery Rev.*, 2014, **79–80**, 172–183.
- 103 M. T. Nelson, *et al.*, Preferential, enhanced breast cancer cell migration on biomimetic electrospun nanofiber ‘cell highways’, *BMC Cancer*, 2014, **14**, 825.
- 104 A. Beliveau, G. Thomas, J. Gong, Q. Wen and A. Jain, Aligned Nanotopography Promotes a Migratory State in Glioblastoma Multiforme Tumor Cells, *Sci. Rep.*, 2016, **6**, 26143.
- 105 P. A. Agudelo-Garcia, *et al.*, Glioma Cell Migration on Three-dimensional Nanofiber Scaffolds Is Regulated by Substrate Topography and Abolished by Inhibition of STAT3 Signaling, *Neoplasia*, 2011, **13**, 831–840.
- 106 D. Liewald, R. Miller, N. Logothetis, H. J. Wagner and A. Schuz, Distribution of Axon Diameters in Cortical White Matter: An Electron-Microscopic Study on Three Human Brains and a Macaque, *Biol. Cybern.*, 2014, **108**, 541–557.
- 107 M. Rabionet, T. Puig and J. Ciurana, Manufacture of PCL scaffolds through electrospinning technology to accommodate Triple Negative Breast Cancer cells culture, *4th CIRP Conf. Biomanufacturing*, 2020, **89**, 98–103.
- 108 V. Gkretsi and T. Stylianopoulos, Cell Adhesion and Matrix Stiffness: Coordinating Cancer Cell invasion and Metastasis, *Front. Oncol.*, 2018, **8**, 145.
- 109 S. S. Rao, *et al.*, Mimicking white matter tract topography using core-shell electrospun nanofibers to examine migration of malignant brain tumors, *Biomaterials*, 2013, **34**, 5181–5190.
- 110 B. D. Cox, M. Natarajan, M. R. Stettner and C. L. Gladson, New concepts regarding focal adhesion kinase promotion of cell migration and proliferation, *J. Cell. Biochem.*, 2006, **99**, 35–52.
- 111 Y. Wang, J. Gong and Y. Yao, Extracellular nanofiber-orchestrated cytoskeletal reorganization and mediated directional migration of cancer cells, *Nanoscale*, 2020, **12**, 3183–3193.
- 112 P. Sharma, K. Sheets, S. Elankumaran and A. S. Nain, The mechanistic influence of aligned nanofibers on cell shape, migration and blebbing dynamics of glioma cells, *Integr. Biol. Quant. Biosci. Nano Macro*, 2013, **5**, 1036–1044.
- 113 Y.-Y. Tseng, J.-Y. Liao, W.-A. Chen, Y.-C. Kao and S.-J. Liu, Sustainable release of carmustine from biodegradable poly[ $[(D,L)]$ -lactide-co-glycolide] nanofibrous membranes in the cerebral cavity: in vitro and in vivo studies, *Expert Opin. Drug Delivery*, 2013, **10**, 879–888.
- 114 Y.-Y. Tseng, *et al.*, Concurrent delivery of carmustine, irinotecan, and cisplatin to the cerebral cavity using biodegradable nanofibers: in vitro and in vivo studies, *Colloids Surf., B*, 2015, **134**, 254–261.
- 115 S. Kuramitsu, K. Motomura, A. Natsume and T. Wakabayashi, Double-edged Sword in the Placement of Carmustine (BCNU) Wafers along the Eloquent Area: A Case Report, *NMC Case Rep. J.*, 2015, **2**, 40–45.

- 116 S. H. Ranganath and C.-H. Wang, Biodegradable micro-fiber implants delivering paclitaxel for post-surgical chemotherapy against malignant glioma, *Biomaterials*, 2008, **29**, 2996–3003.
- 117 M. Irani, G. M. M. Sadeghi and I. Haririan, The sustained delivery of temozolomide from electrospun PCL-Diol-*b*-PU/gold nanocomposite nanofibers to treat glioblastoma tumors, *Mater. Sci. Eng., C*, 2017, **75**, 165–174.
- 118 C. Sun, *et al.*, Noninvasive nanoparticle strategies for brain tumor targeting, *Nanomed. Nanotechnol. Biol. Med.*, 2017, **13**, 2605–2621.
- 119 X. Wei, X. Chen, M. Ying and W. Lu, Brain tumor-targeted drug delivery strategies, *Acta Pharm. Sin. B*, 2014, **4**, 193–201.
- 120 S. H. Ranganath, *et al.*, The use of submicron/nanoscale PLGA implants to deliver paclitaxel with enhanced pharmacokinetics and therapeutic efficacy in intracranial glioblastoma in mice, *Biomaterials*, 2010, **31**, 5199–5207.
- 121 A. Mangraviti, D. Gullotti, B. Tyler and H. Brem, Nanobiotechnology-based delivery strategies: new frontiers in brain tumor targeted therapies, *J. Controlled Release*, 2016, **240**, 443–453.
- 122 M. Irani, G. Mir Mohamad Sadeghi and I. Haririan, Gold coated poly(epsilon-caprolactonediol) based polyurethane nanofibers for controlled release of temozolomide, *Biomed. Pharmacother.*, 2017, **88**, 667–676.
- 123 S. Chen, S. K. Boda, S. K. Batra, X. Li and J. Xie, Emerging Roles of Electrospun Nanofibers in Cancer Research, *Adv. Healthcare Mater.*, 2018, **7**, e1701024.
- 124 W. Liu, S. Thomopoulos and Y. Xia, Electrospun nanofibers for regenerative medicine, *Adv. Healthcare Mater.*, 2012, **1**, 10–25.
- 125 Y. Zhang, C. T. Lim, S. Ramakrishna and Z.-M. Huang, Recent development of polymer nanofibers for biomedical and biotechnological applications, *J. Mater. Sci.: Mater. Med.*, 2005, **16**, 933–946.
- 126 J. Zeng, *et al.*, Influence of the drug compatibility with polymer solution on the release kinetics of electrospun fiber formulation, *J. Controlled Release*, 2005, **105**, 43–51.
- 127 S. Chew, Y. Wen, Y. Dzenis and K. Leong, The Role of Electrospinning in the Emerging Field of Nanomedicine, *Curr. Pharm. Des.*, 2006, **12**(36), 4751.
- 128 X. Qin, 3 - Coaxial electrospinning of nanofibers. in *Electrospun Nanofibers*, ed. Afshari, M., Woodhead Publishing, 2017, pp. 41–71, DOI: [10.1016/B978-0-08-100907-9.00003-9](https://doi.org/10.1016/B978-0-08-100907-9.00003-9).
- 129 D. Han and A. J. Steckl, Triaxial Electrospun Nanofiber Membranes for Controlled Dual Release of Functional Molecules, *ACS Appl. Mater. Interfaces*, 2013, **5**, 8241–8245.
- 130 B. Zhang, C. Li and M. Chang, Curled Poly(ethylene glycol terephthalate)/Poly(ethylene propanediol terephthalate) Nanofibers Produced by Side-by-side Electrospinning, *Polym. J.*, 2009, **41**, 252–253.
- 131 M. Cai, *et al.*, Efficient Synthesis of PVDF/PI Side-by-Side Bicomponent Nanofiber Membrane with Enhanced Mechanical Strength and Good Thermal Stability, *Nanomaterials*, 2018, **9**(1), DOI: [10.3390/NANO9010039](https://doi.org/10.3390/NANO9010039).
- 132 R. Ramachandran, *et al.*, Theranostic 3-Dimensional nano brain-implant for prolonged and localized treatment of recurrent glioma, *Sci. Rep.*, 2017, **7**, 43271.
- 133 X. Xu, X. Chen, Z. Wang and X. Jing, Ultrafine PEG-PLA fibers loaded with both paclitaxel and doxorubicin hydrochloride and their in vitro cytotoxicity, *Eur. J. Pharm. Biopharm.*, 2009, **72**, 18–25.
- 134 N. Nikmaram, *et al.*, Emulsion-based systems for fabrication of electrospun nanofibers: food, pharmaceutical and biomedical applications, *RSC Adv.*, 2017, **7**, 28951–28964.
- 135 X. Luo, *et al.*, Antitumor activities of emulsion electrospun fibers with core loading of hydroxycamptothecin via intratumoral implantation, *Int. J. Pharm.*, 2012, **425**, 19–28.
- 136 T. Okuda, Y. Tahara, N. Kamiya, M. Goto and S. Kidoaki, S/O-nanodispersion electrospun fiber mesh effective for sustained release of healthy plasmid DNA with the structural and functional integrity, *J. Biomater. Sci., Polym. Ed.*, 2013, **24**, 1277–1290.
- 137 H. S. Yoo, T. G. Kim and T. G. Park, Surface-functionalized electrospun nanofibers for tissue engineering and drug delivery, *Adv. Drug Delivery Rev.*, 2009, **61**, 1033–1042.
- 138 S. Thakkar and M. Misra, Electrospun polymeric nanofibers: new horizons in drug delivery, *Eur. J. Pharm. Sci.*, 2017, **107**, 148–167.
- 139 E. J. Falde, *et al.*, Layered Superhydrophobic Meshes for Controlled Drug Release, *J. Controlled Release*, 2015, **214**, 23–29.
- 140 T. Okuda, K. Tominaga and S. Kidoaki, Time-programmed dual release formulation by multilayered drug-loaded nanofiber meshes, *J. Controlled Release*, 2010, **143**, 258–264.
- 141 Z. Zhang, *et al.*, Time-programmed DCA and oxaliplatin release by multilayered nanofiber mats in prevention of local cancer recurrence following surgery, *J. Controlled Release*, 2016, **235**, 125–133.
- 142 X. Xu, *et al.*, BCNU-loaded PEG-PLLA ultrafine fibers and their in vitro antitumor activity against Glioma C6 cells, *J. Controlled Release*, 2006, **114**, 307–316.
- 143 S. T. Yohe, V. L. M. Herrera, Y. L. Colson and M. W. Grinstaff, 3D Superhydrophobic Electrospun Meshes as Reinforcement Materials for Sustained Local Drug Delivery Against Colorectal Cancer Cells, *J. Controlled Release*, 2012, **162**(1), 92–101.
- 144 E. Yan, *et al.*, Biocompatible core-shell electrospun nanofibers as potential application for chemotherapy against ovary cancer, *Mater. Sci. Eng., C*, 2014, **41**, 217–223.
- 145 S. Liu, *et al.*, Inhibition of orthotopic secondary hepatic carcinoma in mice by doxorubicin-loaded electrospun polylactide nanofibers, *J. Mater. Chem. B*, 2012, **1**, 101–109.
- 146 H. Brem, Polymers to treat brain tumours, *Biomaterials*, 1990, **11**, 699–701.
- 147 A. Bregy, *et al.*, The role of Gliadel wafers in the treatment of high-grade gliomas, *Expert Rev. Anticancer Ther.*, 2013, **13**, 1453–1461.
- 148 J. M. Gallego, J. A. Barcia and C. Barcia-Marino, Fatal outcome related to carmustine implants in glioblastoma multiforme, *Acta Neurochir Wien*, 2007, **149**, 261–265; discussion 265 .

- 149 F. Mu, *et al.*, Tumor resection with carmustine wafer placement as salvage therapy after local failure of radiosurgery for brain metastasis, *J. Clin. Neurosci.*, 2015, **22**, 561–565.
- 150 D. Han, *et al.*, Multi-layered core-sheath fiber membranes for controlled drug release in the local treatment of brain tumor, *Sci. Rep.*, 2019, **9**, 17936.
- 151 D. Han, *et al.*, *In vitro* evaluation of MPA-loaded electrospun coaxial fiber membranes for local treatment of glioblastoma tumor cells, *J. Drug Delivery Sci. Technol.*, 2017, **40**, 45–50.
- 152 S.-F. Chou and D. Carson, & Woodrow, K. A. Current strategies for sustaining drug release from electrospun nanofibers, *Sel. Contrib. 17th Int. Symp. Recent Adv. Drug Deliv. Syst. Salt Lake City USA*, 2015, **220**, 584–591.
- 153 D. Demir, D. Güreş, T. Tecim, R. Genç and N. Bölgen, Magnetic nanoparticle-loaded electrospun poly( $\epsilon$ -caprolactone) nanofibers for drug delivery applications, *Appl. Nanosci.*, 2018, **8**, 1461–1469.
- 154 K. Qiu, *et al.*, Doxorubicin-loaded electrospun poly(L-lactic acid)/mesoporous silica nanoparticles composite nanofibers for potential postsurgical cancer treatment, *J. Mater. Chem. B*, 2013, **1**, 4601–4611.
- 155 M. Chen, *et al.*, Antitumor efficacy of a PLGA composite nanofiber embedded with doxorubicin@MSNs and hydroxycamptothecin@HANPs, *RSC Adv.*, 2014, **4**, 53344–53351.
- 156 C. Imashiro, *et al.*, Development of accurate temperature regulation culture system with metallic culture vessel demonstrates different thermal cytotoxicity in cancer and normal cells, *Sci. Rep.*, 2021, **11**, 21466.
- 157 T.-C. Lin, F.-H. Lin and J.-C. Lin, *In vitro* feasibility study of the use of a magnetic electrospun chitosan nanofiber composite for hyperthermia treatment of tumor cells, *Acta Biomater.*, 2012, **8**, 2704–2711.
- 158 Effect of Local Hyperthermia on Blood Flow and Microenvironment: A Review | Cancer Research, [https://cancerres.aacrjournals.org/content/44/10\\_Supplement/4721s.short](https://cancerres.aacrjournals.org/content/44/10_Supplement/4721s.short).
- 159 M. M. Yallapu, *et al.*, Multi-functional magnetic nanoparticles for magnetic resonance imaging and cancer therapy, *Biomaterials*, 2011, **32**, 1890–1905.
- 160 A. GhavamiNejad, *et al.*, Mussel-Inspired Electrospun Smart Magnetic Nanofibers for Hyperthermic Chemotherapy, *Adv. Funct. Mater.*, 2015, **25**, 2867–2875.
- 161 Y.-J. Kim, M. Ebara and T. Aoyagi, A Smart Hyperthermia Nanofiber with Switchable Drug Release for Inducing Cancer Apoptosis, *Adv. Funct. Mater.*, 2013, **23**, 5753–5761.
- 162 A. Jain, *et al.*, Guiding Intracortical Brain Tumour Cells to an Extracortical Cytotoxic Hydrogel Using Aligned Polymeric Nanofibres, *Nat. Mater.*, 2014, **13**, 309–316.
- 163 M. Cristofanilli, *et al.*, Circulating tumor cells, disease progression, and survival in metastatic breast cancer, *N. Engl. J. Med.*, 2004, **351**, 781–791.
- 164 P. S. Steeg, Tumor metastasis: mechanistic insights and clinical challenges, *Nat. Med.*, 2006, **12**, 895–904.
- 165 C. L. Sawyers, The cancer biomarker problem, *Nature*, 2008, **452**, 548–552.
- 166 S. Sharma, *et al.*, Circulating Tumor Cell Isolation, Culture, and Downstream Molecular Analysis, *Biotechnol. Adv.*, 2018, **36**, 1063–1078.
- 167 S. N. Shishido, *et al.*, Circulating tumor cells as a response monitor in stage IV non-small cell lung cancer, *J. Transl. Med.*, 2019, **17**, 294.
- 168 J. B. Smerage, *et al.*, Circulating Tumor Cells and Response to Chemotherapy in Metastatic Breast Cancer: SWOG S0500, *J. Clin. Oncol.*, 2014, **32**, 3483–3489.
- 169 M. Cristofanilli, *et al.*, Circulating tumor cells: a novel prognostic factor for newly diagnosed metastatic breast cancer, *J. Clin. Oncol.*, 2005, **23**, 1420–1430.
- 170 M. C. Miller, G. V. Doyle and L. W. M. M. Terstappen, Significance of Circulating Tumor Cells Detected by the CellSearch System in Patients with Metastatic Breast Colorectal and Prostate Cancer, *J. Oncol.*, 2010, **2010**, 617421.
- 171 J. S. de Bono, *et al.*, Circulating Tumor Cells Predict Survival Benefit from Treatment in Metastatic Castration-Resistant Prostate Cancer, *Clin. Cancer Res.*, 2008, **14**, 6302–6309.
- 172 S. J. Cohen, *et al.*, Relationship of circulating tumor cells to tumor response, progression-free survival, and overall survival in patients with metastatic colorectal cancer, *J. Clin. Oncol.*, 2008, **26**, 3213–3221.
- 173 M. W. Lee, G. H. Kim, H. K. Jeon and S. J. Park, Clinical Application of Circulating Tumor Cells in Gastric Cancer, *Gut Liver*, 2019, **13**, 394–401.
- 174 M. G. Krebs, *et al.*, Evaluation and prognostic significance of circulating tumor cells in patients with non-small-cell lung cancer, *J. Clin. Oncol.*, 2011, **29**, 1556–1563.
- 175 D. R. Shaffer, *et al.*, Circulating tumor cell analysis in patients with progressive castration-resistant prostate cancer, *Clin. Cancer Res.*, 2007, **13**, 2023–2029.
- 176 J. Xue, D. Pisignano and Y. Xia, Maneuvering the Migration and Differentiation of Stem Cells with Electrospun Nanofibers, *Adv. Sci.*, 2020, **7**(15), 2000735.
- 177 B. S. Miller, K. K. Briggs, B. Downie and J. R. Steadman, Clinical Outcomes following the Microfracture Procedure for Chondral Defects of the Knee: A Longitudinal Data Analysis, *Cartilage*, 2010, **1**, 108–112.
- 178 V. Musella, *et al.*, Circulating tumor cells as a longitudinal biomarker in patients with advanced chemorefractory, RAS-BRAF wild-type colorectal cancer receiving cetuximab or panitumumab, *Int. J. Cancer*, 2015, **137**, 1467–1474.
- 179 S. Riethdorf, *et al.*, Detection of circulating tumor cells in peripheral blood of patients with metastatic breast cancer: a validation study of the CellSearch system, *Clin. Cancer Res.*, 2007, **13**, 920–928.
- 180 C. Alix-Panabières and K. Pantel, Challenges in circulating tumour cell research, *Nat. Rev. Cancer*, 2014, **14**, 623–631.
- 181 I. Desitter, *et al.*, A new device for rapid isolation by size and characterization of rare circulating tumor cells, *Anti-cancer Res.*, 2011, **31**, 427–441.
- 182 P. Gogoi, *et al.*, Development of an Automated and Sensitive Microfluidic Device for Capturing and Characterizing Circulating Tumor Cells (CTCs) from Clinical Blood Samples, *PLoS One*, 2016, **11**(1), e0147400.
- 183 P. Paterlini-Brechot and N. L. Benali, Circulating tumor cells (CTC) detection: clinical impact and future directions, *Cancer Lett.*, 2007, **253**, 180–204.

- 184 N. J. Nelson, Circulating Tumor Cells: Will They Be Clinically Useful?, *JNCI, J. Natl. Cancer Inst.*, 2010, **102**, 146–148.
- 185 H. Geckil, F. Xu, X. Zhang, S. Moon and U. Demirci, Engineering hydrogels as extracellular matrix mimics, *Nanomed.*, 2010, **5**, 469–484.
- 186 N. Zhang, *et al.*, Electrospun TiO<sub>2</sub> Nanofiber-Based Cell Capture Assay for Detecting Circulating Tumor Cells from Colorectal and Gastric Cancer Patients, *Adv. Mater.*, 2012, **24**, 2756–2760.
- 187 G. Yang, *et al.*, Capturing Circulating Tumor Cells through a Combination of Hierarchical Nanotopography and Surface Chemistry, *ACS Biomater. Sci. Eng.*, 2018, **4**, 2081–2088.
- 188 H. Liu, *et al.*, Capture and release of cancer cells using electrospun etchable MnO<sub>2</sub> nanofibers integrated in microchannels, *Appl. Phys. Lett.*, 2015, **106**, 093703.
- 189 C.-C. Yu, *et al.*, Random and aligned electrospun PLGA nanofibers embedded in microfluidic chips for cancer cell isolation and integration with air foam technology for cell release, *J. Nanobiotechnol.*, 2019, **17**, 31.
- 190 L. Zhao, *et al.*, High-Purity Prostate Circulating Tumor Cell Isolation by a Polymer Nanofiber-Embedded Microchip for Whole Exome Sequencing, *Adv. Mater. Deerfield Beach Fla.*, 2013, **25**, 2897–2902.
- 191 S. Hou, *et al.*, Polymer Nanofiber-Embedded Microchips for Detection, Isolation, and Molecular Analysis of Single Circulating Melanoma Cells, *Angew. Chem., Int. Ed.*, 2013, **52**(12), 3379–3383.
- 192 L. A. Diaz and A. Bardelli, Liquid Biopsies: Genotyping Circulating Tumor DNA, *J. Clin. Oncol.*, 2014, **32**, 579–586.
- 193 E. S. Lianidou, Circulating Tumor Cell Isolation: A Marathon Race Worth Running, *Clin. Chem.*, 2014, **60**, 287–289.
- 194 K. Pantel and C. Alix-Panabières, Circulating tumour cells in cancer patients: challenges and perspectives, *Trends Mol. Med.*, 2010, **16**, 398–406.
- 195 A. Senthamizhan, B. Balusamy and T. Uyar, Recent progress on designing electrospun nanofibers for colorimetric biosensing applications, *Futur. Biomed. Eng. Bioeng. Organoids Tissue Dev. Biomater. Biosens.*, 2020, **13**, 1–8.
- 196 B. Muz, P. de la Puente, F. Azab and A. K. Azab, The role of hypoxia in cancer progression, angiogenesis, metastasis, and resistance to therapy, *Hypoxia Auckl. NZ*, 2015, **3**, 83–92.
- 197 R. Xue, M. T. Nelson, S. A. Teixeira, M. S. Viapiano and J. J. Lannutti, Cancer cell aggregate hypoxia visualized in vitro via biocompatible fiber sensors, *Biomaterials*, 2016, **76**, 208–217.
- 198 Y. Zhang, *et al.*, Electrospun bimetallic Au-Ag/Co<sub>3</sub>O<sub>4</sub> nanofibers for sensitive detection of hydrogen peroxide released from human cancer cells, *Anal. Chim. Acta*, 2018, **1042**, 20–28.
- 199 X. Wang, *et al.*, Novel electrochemical biosensor based on functional composite nanofibers for sensitive detection of p53 tumor suppressor gene, *Anal. Chim. Acta*, 2013, **765**, 63–69.
- 200 S. Thakkar and M. Misra, Electrospun polymeric nanofibers: new horizons in drug delivery, *Eur. J. Pharm. Sci.*, 2017, **107**, 148–167.
- 201 E. J. Torres-Martinez, J. M. Cornejo Bravo, A. Serrano Medina, G. L. Pérez González and L. J. Villarreal Gómez, A Summary of Electrospun Nanofibers as Drug Delivery System: Drugs Loaded and Biopolymers Used as Matrices, *Curr. Drug Delivery*, 2018, **15**, 1360–1374.